miR-193b-3p Promotes Proliferation of Goat Myoblast Through Directly Targeting IGF2BP1 and Activating Its Transcription

Li Li
Sichuan Agricultural University - Chengdu Campus
Xiao Zhang
Sichuan Agricultural University - Chengdu Campus
Hailong Yang
Sichuan Agricultural University
Xiaoli Xu
Sichuan Agricultural University - Chengdu Campus
Yuan Chen
Sichuan Agricultural University - Chengdu Campus
Dinghui Dai
Sichuan Agricultural University
Siyuan Zhan
Sichuan Agricultural University - Chengdu Campus
Jiazhong Guo
Sichuan Agricultural University - Chengdu Campus
Tao Zhong
Sichuan Agricultural University
Linjie Wang
Sichuan Agricultural University
Jiaxue Cao
Sichuan Agricultural University
Hongping Zhang (zhp@sicau.edu.cn)
Sichuan Agricultural University https://orcid.org/0000-0001-8290-7041

Research

Keywords: miR-193b-3p, IGF2BP1, microRNA, nucleus, transcriptional activation, enhancer

Posted Date: October 23rd, 2020

DOI: https://doi.org/10.21203/rs.3.rs-95708/v1

Abstract

Background

As a well-known cancer-related miRNA, miR-193b-3p is enriched in skeletal muscle but dysregulated in muscle disease. However, mechanism underpinning has not been addressed so far.

Methods

Here, we probed the impact of miR-193b-3p on myogenesis by mainly using goat tissues and skeletal muscle satellite cells (MuSCs), with combined methods including RNA-seq to profile the transcriptome affected by miR-193b-3p, cell-counting kit-8 (CCK-8) and 5-ethynyl-2'-deoxyuridine (EdU) for cell proliferation assay, and RNA-RNA dual-labeled fluorescence in situ hybridization (FISH) for RNA colocalization.

Results

miR-193b-3p is highly enriched in goat skeletal muscles, and ectopic miR-193b-3p promotes MuSCs proliferation and differentiation. Moreover, insulin-like growth factor-2 mRNA-binding protein 1 (IGF2BP1) is the most activated insulin signaling genes when overexpression miR-193b-3p and the miRNA recognition element (MRE) within IGF1BP1 3′ untranslated region (UTR) is indispensable for its activation caused by miR-193b-3p. Consistently, expression patterns and function of IGF2BP1 were similar to those of miR-193b-3p in tissues and MuSCs. While the overexpression of miR-193b-3p failed to induce pax7 expression and myoblast proliferation when IGF2BP1 knockdown. Furthermore, miR-193b-3p destabilized IGF2BP1 mRNA but unexpectedly promoted levels of IGF2BP1 heteronuclear RNA (hnRNA) dramatically. Moreover, miR-193b-3p could enhance fly luciferase activity when inserted upstream of its promoter, and induce neighboring genes of itself. However, miR-193b-3p inversely regulated IGF2BP1 and myoblast proliferation in mouse C2C12 myoblast. These data unveil that goat miR-193b-3p promotes myoblast proliferation via activating IGF2BP1 by binding on its 3′ UTR.

Conclusions

Our novel findings highlight the positive regulation between miRNA and its target genes in muscle development, which further extends the repertoire of miRNA functions.

Background

Formation of skeletal muscle (myogenesis) is a complex program covering the embryonic stage driven by myogenic progenitor cells [1] and the postnatal phase mainly contributed by skeletal muscle satellite cells (MuSCs). MuSCs govern myofiber number increase (hyperplasia), size enlargement (hypertrophy), and regeneration [2] through sequential progress including proliferation, differentiation, and fusion of myoblasts [3], in which several protein-coding genes *play critical roles*, such as paired box 7 (Pax7), proliferating cell nuclear antigen (PCNA) [4], myogenic regulatory factors (MRFs) like myogenic differentiation protein 1 (MyoD) and myogenin (MyoG) [5], myomaker *[3], as well as insulin-like growth factor family [6].*

As highly evolutionary conserved small endogenous non-coding RNAs, microRNAs (miRNAs, ~ 22-nucleotide long) drives fundamental cellular processes like proliferation and differentiation through fine-tune gene enrichment [7]. Especially the function and mechanism of several exclusively expressed muscle miRNAs (myomiRs), including miR-1/miR-206 and miR-133 families, have been well documented in myogenesis [8, 9]. Nevertheless, except for these muscle-specific miRNAs, some ubiquitously expressed tumor-related miRNAs like miR-125b [10] and miR-223 [11] also play essential roles in myogenesis [12-14].

As a well-accepted anti-tumor oncogene, miR-193b generally targets and negatively regulates genes involving cell cycle [15, 16], though miR-193b is markedly downregulated [17-19] or dramatically elevated in some cancers [20, 21]. Outstandingly, miR-193b is usually dysregulated in muscle diseases like Duchenne muscular dystrophy (DMD) [22, 23], and miR-193b governs the transition between myoblasts and brown adipocytes [24, 25]. These suggest that the function of miR-193b-3p in myogenesis remains to be systematically illustrated.

Typically, miRNAs negatively regulate gene expression through miRNA-mRNA interaction [7], e.g., miRNAs bind complementary target RNAs and trigger the destruction of targeted mRNA (a majority, >84%)[26] or block translation (11–16%) [27]. Nevertheless, recently accumulating evidence support that cytoplasmic miRNAs can also activate gene expression unconventionally through enhancing the translation by seed-matching binding on 5′ [28] or 3′ untranslated region (UTR) [29], or even non-seed-matching sites in the 5′ UTR of mRNAs [30]. Meanwhile, nucleus-located miRNAs mediates gene activation epigenetically via targeting enhancers [31] or targeting the 5′ -end of gene [32]. Undoubtedly, the functional significance of the activating miRNAs in animal normal development remains largely undetermined.

Here, mainly using tissues and MuSCs from goat, we found out that miR-193b-3p is located in enhancer loci and enriched in skeletal muscle. Furthermore, the insulin-like growth factor-2 mRNA-binding protein 1 (IGF2BP1), an anti-apoptotic gene, certainly promotes cell proliferation [33, 34] and is directly targeted and activated by miR-193b-3p transcriptionally via seed-matching sites in the 3′ UTR. Besides, the miR-193b-3p /IGF2BP1 axis mainly promotes myoblast proliferation. Our research provides a novel mechanism of miRNA activating its targeting gene transcriptionally.

Methods

Ethics declarations

All experimental protocols present here were strictly conducted following the Regulations for the Administration of Affairs Concerning Experimental Animals (Ministry of Science and Technology, China), and entirely approved by the Animal Care and Use Committee, Sichuan Agricultural University.

Animals and samples collection

A total of 12 female goat fetuses and kids aged 45, 60, and 105 days of gestation, and 3 days postnatal (n = 3 per stage) were randomly chosen and humanely sacrificed at the Jianzhou Big-Eared goats farm (Sichuan province, China). Tissue samples from six organs, including heart, liver, lung, spleen, kidney, and longissimus dorsi (LD) muscle were quickly collected and snap-frozen in liquid nitrogen for further study.

Isolating goat MuSCs

We successfully isolated MuSCs from LD muscles of neonatal goats using the typical protocols described previously [62]. Briefly, sampled LD muscle blocks were quickly washed with sterile phosphate-buffered saline (PBS, Hyclone), minced with ophthalmic scissors, digested in 0.2% Pronase at 37 °C for 1 h (Sigma-Aldrich), centrifuged at 1 500 ×g for 6 min to get the pellet. The pellets were sequentially suspended (Dulbecco's modified Eagle's medium supplemented with 15% fetal bovine serum, Hyclone), filtered (70-μm-mesh sieve, BD), span (800 ×g for 5 min) to isolate MuSCs. Using a Percoll gradient (90, 40, and 20%) (Sigma-Aldrich), we enriched isolated MuSCs in between 40% and 90% in the Percoll interface. Then the enriched MuSCs were subsequently validated by immunostaining with an antibody for Pax7 (Paired box 7, rabbit anti-Pax7, 1:100 dilution, Boster), a critical marker for MuSCs. Finally, the purified $Pax7^+$ MuSCs were stored in liquid nitrogen.

Cell culture and transfection

Cells were in general cultured in a 5% CO_2 atmosphere at 37 °C. MuSCs were initially seeded in 6-well (~2×10^5 cells per well) or 12-well (~1×10^5 cells per well) plates in growth medium (GM) that contains DMEM plus 10% fetal bovine serum (FBS, Gibco, USA) and 2% Penicillin & Streptomycin (Invitrogen, USA) solution, when amounted to 80%–90% confluency, GM was replaced by differentiation medium (DM) via reducing FBS from 10% to 2% to induce differentiation. The medium was refreshed every 2 d.

For the gain and loss function study, when cells at 80%~90% confluence, the GM was replaced with DMEM supplemented with 10% FBS. Then cells were transfected using Lipofectamine 3000 (Invitrogen, USA) with interfering RNA (si-NC, in-193b-3p and siIGF2BP1) or overexpression plasmid (pCtrl/pIGF2BP1) and chi-miR-193b-3p mimic (mi-193b-3p, RiboBio, China) at indicative concentrations, according to the manufacturer's direction. The transfected cells were kept in GM or replaced with DMEM

supplemented with 2% FBS to induce differentiation and collected for RNA/protein assay at 48 h and immunofluorescence stained with EdU at indicative time points, or with MyHC (Myosin Heavy Chain) antibody at 7^{th} d post differentiation.

Given that culturing cells are easily contaminated by mycoplasma, which leads to severely spurious results, we monitored and even employed polymerase chain reaction (PCR) to directly detect mycoplasma contamination (TRansgen Biotech, China) in culturing media before transfection and harvesting [63], to ensure cells were mycoplasma-free (Supp Fig.4B).

Reporter constructs and luciferase assays

To evaluate the targeting relationship between *IGF2BP1* and miR-193b-3p based on the potential MRE (miRNA recognition element) of miR-193b-3p within 3 UTR regions of IGF2BP1 mRNA predicted with online software FINDTAR3 (http://bio.sz.tsinghua.edu.cn/) and BIBIServ2 (https://bibiserv.cebitec.uni-bielefeld.de/rnahybrid/), a 470 bp-length fragment 3 UTR regions of IGF2BP1 mRNA containing the wild-type (wt, GGCCGG) or mutant (mut, GTAAAG) were synthesized and cloned into the psiCHECK-2 vector (Promega) to generate IGF2BP1-wt and IGF2BP1-mut vectors (Sangon Biotech, China), respectively.

To detect the enhancer activity of miR-193b-3p, two fragments harboring goat miR-193b-3p (5 -ggtaccGTTTATGTTTTATCCAACTGGCCCACAAAGTCCCGCTTTTGGGGTCATTCTAGACGGCGAGGGATTCAGctcgag-3) and miR-193b-5p (5-ggtaccGGAGGCTGTGGTCCCAGAATCGGGGTTTTGAGGGCGAGATGAGTTTATGTTTTATCCctcgag-3) were successfully amplified and subcloned into the pGL3 Promoter vector (Promega, USA) between the KpnI and XhoI sites. These constructs were cotransfected with pRLT-K (Promega, USA) encoding for the renilla luciferase gene to measure their transfection efficiency.

For the luciferase reporter assays, goat MuSCs (~1×10^4 cells per well), mouse C2C12 myoblasts (1×10^5 cells per well, Thermo, USA), and HeLa cells (~2×10^5 cells per well, ATCC, USA) were cultured in GM on 24-well plates and cotransfected with vectors (640 ng/well for each vector) using Lipofectamine 2000 reagent when cells were grown to 80 %–90 % confluence. After transfection for 48 h, the transfected cells were lysed, and the activities of firefly and Renilla luciferase were measured using a dual-luciferase reporter assay system (Promega, USA), according to the user's guidelines.

Overexpressing and interfering plasmids construct

To produce IGF2BP1 and miR-193b-3p overexpressing vector, we amplified the coding sequence (CDS) of IGF2BP1 (XM_005693695.3) (forward primer 5-CCCAAGCTTATGAACAAGCTGTACATCGG; reverse primer 5 -CCGGAATTCTCACTTCCTCCGGGCCTGGGC, 1734 bpfrom cDNA and 371 bp region of the miR-193b-3p gene (forward primer 5 -CCCAAGCTTACTGTTCTCCCGTCATTCC -3; the reverse primer 5 - CCGGAATTCGTAGCAAACCTCCCCTCTT -3) from the goat genome. Then subcloned them into the pcDNA 3.1(+) vector separately by using double digestion with Hind and EcoRI, and T4 DNA ligase (Invitrogen, USA) according to the manufacturer's guidelines. PCR combining with Sanger sequencing was performed to validate the target gene.

To provide solid interfering results for IGF2BP1, three small interfering RNA, including siRNA1, CAGCTCCTTTATGCAGGCT; siRNA2, CTCCTTTATGCAGGCTCCA; and siRNA3 CTTTATGCAGGCTCCAGAG, targeting goat IGF2BP1 mRNA were designed and synthesized in RiboBio (Guangzhou, China). We transfected them separately into MuSCs at two concentrations (50 nM and 100 nM) and then quantified IGF2BP1 mRNAs. The results suggest that IGF2BP1 levels are efficiently decreased at 100 nM for each siRNA (Supp Fig. 6), thus in the following experiment, we pooled them at 100 nM concentration. Besides, the miR-193b-3p miRNA mimic (mi-193b-3p) and control (mi-Ctrl), as well as inhibitor (in-193b-3p) and control (in-Ctrl) were ordered from RiboBio (Guangzhou, China).

RNA extraction and qPCR

Following the manufacturer's instruction, total RNAs were extracted from tissues or cultured cells using RNAiso Plus reagent (TaKaRa, Japan), and roughly qualified by using 1.5% agarose gels electrophoresis and NanoDrop 2000c Spectrophotometer. Then the qualified RNAs (~1 mg) were reversely transcribed into cDNA by using the PrimeScript™ RT reagent Kit with gDNA Eraser or miRNA PrimeScript RT reagent Kit (Takara, Japan) separately for mRNA or miRNA assay. Then according to the

manufacturer's guide, RNA levels of target genes in these cDNA were accurately measured by using real-time PCR (RT-qPCR) in the Bio-Rad CFX96 system (Bio-Rad, USA) with SYBR Premix Ex TaqTM II (Takara, Japan). Each treatment performed at least triply three independent times, and each sample triplicates in qPCR. Moreover, to enhance the accuracy, three housekeeping genes in goat ACTB (*Actin Beta)*, *SDHA (Succinate Dehydrogenase Complex Flavoprotein Subunit A),* and *PGK1(Phosphoglycerate Kinase 1))* and mouse (ACTB, *GAPDH*, and *Hprt (Hypoxanthine Phosphoribosyltransferase 1))* were used as an internal control. The $2^{-\triangle\triangle Ct}$ or $2^{-\triangle Ct}$ methods were employed to calculate the relative RNA levels of target genes. The detailed information for primers was listed in Supplementary Table 1.

Western Blotting and Immunofluorescence for protein analyses

To analyze protein levels of the target genes via western blotting (WB), we extracted total proteins in lysed cells by using radioimmunoprecipitation assay (RIPA) (Beyotime, China). After quantified through the bicinchoninic acid (BCA) method (Beyotime, China), protein samples (~20 μg) were sequentially loaded for electrophoresis, transferred on polyvinylidene fluoride (PVDF) membranes (Millipore, USA), incubated with primary antibodies for IGF2BP1, MyoG, MyoD, and PAX3 (Abcam, UK) at 4 °C overnight and secondary IgG (Beyotime, China) for 2 h. After the addition of horseradish peroxidase (HRP) substrate, protein bands were exposed via electrochemiluminescence (ECL) (Pierce, USA) and analyzed by using Image Software. GAPDH (BOSTER, China) worked as a loading control.

For immunofluorescence assay, MuSCs (seeded in 3.5-cm Petri dishes with ~2×10^4 cells per dish) cultured in DM for 7 days were fixed with 4% paraformaldehyde (room temperature, 15 min), washed with 1 mL PBS (3 times), permeabilized with 1 mL 0.5% Triton X-100 (4 °C, 10 min), blocked in 1 mL 2% bovine serum albumin (37 °C, 30 min), incubated with anti-mouse Myosin heavy chain (MyHC) (1: 200, 4 °C, overnight) (R&D Systems, USA) and secondary antibodies Cy3_IgG (H + L) (1: 200, Solarbio, Shanghai, China) 37 °C for 2 h sequentially. Finally, 0.05μg/mL DAPI (4', 6'-diamidino-2-phenylindole; Invitrogen) were added to cells and kept in the dark (37 °C for 10 min). Images were captured by using an Olympus IX53 inverted microscope (Tokyo, Japan), and then analyzed by using ImageJ software.

CCK-8 assay for cell proliferation

Cells were inoculated in 96-well plates with 2×10^3 cells per well initially (~ 30% confluency) and cultured in GM for 2 days, then transfected with different vectors according to protocols described above. Every 24 h, the absorbance value for each sample was measured at 450 nm by using a Microplate Reader (Model 680, Bio-Rad) after added 10 μL of Cell-Counting Kit-8 (CCK-8) reagents (Kumamoto, Japan) to the cells for 2 h.

EdU assays for cell proliferation

MuSCs (2×10^3 cells per well) were initially cultured and transfected the same as in CCK-8 assay. Twelve hours after transfection, primary myoblasts were cultured in GM consisting of 10 μM 5-ethynyl-2'-deoxyuridine (EdU; RiboBio China). Every 24 h, the cells were fixed (4% PFA at room temperature for 30 min), permeabilized (0.5% Triton X-100), incubated (1 × Apollo reaction cocktail for 30min), and then stained (1 × Hoechst 33342 for 30 min). Finally, we quantified the EdU-stained cells (ratio of EdU^+ myoblasts to all) using randomly selected fields captured shortly after staining by employing an Olympus IX53 inverted microscope (Tokyo, Japan). Assays were performed at least three times.

Dual-labeled Fluorescence in Situ Hybridization (RNA-RNA FISH)

To detect the spatial localization of IGF2BP1 and miR-193b-3p RNA, the Cy5- labeled fluorescence oligonucleotide probes complementary to goat IGF2BP1 mRNA (5′-GCCGGATTTGACCAAGAACTGGCCGCTGTAGGA-3′, red) and FAM-labeled chi-miR-193b-3p probes (5′-AGCGGGACTTTGTGGGCCAGTT-3′, green) were synthesized (Servicebio, China). MuSCs proliferating for 2 d and differentiating for 7 d were rinsed with PBS (5 min), fixed in 4% DEPC-treated paraformaldehyde (room temperature, 10 min), permeated in PBS supplemented with 0.5% Triton (4 ℃, 5 min), and washed 3 times ×5 min with PBS (PH 7.4). Then the FISH experiments were performed in a dark environment with the following procedures. For each well, added 200 μL pre-hybridized solution (37 ℃, 30 min), hybridized with 8 ng/μL probe in 50 μL buffer (2× SSC, 10% formamide, 10% dextran sulfate) at 37 ℃ overnight. The cells were sequentially washed with a hybridized solution I, II, and III at 42℃ 3 times ×5 min, 1 time, and 1 time,

and finally stained with 0.05μg/ mL DAPI (Invitrogen) at 37℃ for 10 min, washed with PBS 3 times ×5 min, and sealed with 25% glycerin.

Images were captured less than 5 h after hybridization by using Nikon DS-U3 in Nikon Eclipse Ti-SR and then analyzed by employing the CaseViewer software.

Nuclear-cytoplasmic fractionation

To accurately quantify expression levels of the target genes in the cytoplasm and nuclear separately, MuSCs proliferating for 2 d and differentiating for 7 d were fractionated into nuclear/cytoplasmic parts by using Nuclear/cytoplasmic fractionation & Nuclear RNA Purification Kit (Norgen Biotek, Canada), as described before [64]. In brief, the total RNA was separately extracted from both the supernatant (cytosol fraction) and pellet (nuclei), retro-transcribed into cDNA, and quantified targeted genes by using RT-qPCR. The nuclear-enriched U6 and cytoplasm-enriched 18S were used as control.

ActD analysis

According to methods described previously [65], we analyzed the effect of miR-193b-3p on IGF2BP1 mRNA stability by using actinomycin D (ActD, Sigma) to block newly mRNA synthesis. In general, MuSCs were cultured in 12-well (~1×10^5 cells per well) plates and separately transfected with miR-193b-3p mimic, mimic NC, inhibitor, and inhibitor NC for 24 h. Then cells were treated with actinomycin D (5 μg/ml) and harvested at 0, 60, and 120 min post-treated. The total RNA was extracted from each sample and finally, the remaining levels of IGF2BP1 mRNA were quantified by using the canonical RT-qPCR method. At least each treatment contained three independent biological repetitions.

mRNA-seq and bioinformatic analyses

Library preparation and poly(A) selection mRNA-seq was performed at Novogene Company (Beijing, China). Briefly, using NEBNext® UltraTM RNA Library Prep Kit Illumina®, qualified total RNA samples (200 ng) extracted from cells transfected with miR-193b-3p mimic or control (n=4 per group) were used to isolate polyA fraction (mRNA), following by fragmentation and generation of double-stranded cDNA. Libraries were sequentially evaluated by Qubit 2.0 Fluorometer, Agilent 2100 bioanalyzer, and RT-qPCR. Then qualified libraries were sequenced in Illumina HiSeq 2500 platform ((Illumina, USA) with a 2x150 bp pair-end.

The raw data of each sample were filtered to obtain the clean data (>8 Gb per sample), then amount to 97.09▯▯97.37▯ clean reads were quickly and accurately mapped onto the Capra_hircus _ARS1 reference genome (ftp://ftp.ncbi.nlm.nih.gov/genomes/all/GCF/001/704/415/GCF_001704415.1_ARS1/GCF_001704415.1_ARS1_genomic.fna.gz) using HISAT2, among which as high as 93.94▯▯94.3▯ clean reads were uniquely mapped. The read count for each one was calculated using fragments per kilobase of transcript sequence per million base pairs sequenced (FPKM) value to evaluate gene expression. Differentially expressed genes (DEGs) between samples were canonically identified by DESeq2 R package vision 1.16.1 (|log2(FoldChange)| > 0 & padj < 0.05) [66].

Transcriptome clustering based on principal component analysis (PCA) indicates that miR_193b-3p mimics or control (mi-Ctrl)-treated cells are distinctly separated. Function Enrichment Analyses of DEGs, including Gene Ontology (GO) enrichment analysis and KEGG pathway, were implemented by using the DESeq2 with P-adj < 0.05 (adjusted via Benjamini-Hochberg) was considered significantly enriched.

Statistical analysis

Unless stated otherwise, data presented here are shown as mean ± SD (standard deviation) from at least triplicate independent samples or animals. The unpaired two-tailed t-test in Graphpad Prism 7 was employed to evaluate means' difference, with significant threshold value set at ***$P < 0.001$▯**$P < 0.01$, *$P < 0.05$, and § P < 0.1.

Results

miR-193b-3p promotes myogenesis of goat MuSC

According to the human genome (GRCh38/hg38, UCSC Genome Browser), miR193BHG (MIR193B host gene) locates on human chr16 and exhibits high sequence conservation among species. Notably, the 22-nt nucleotide sequence of miR-193b-3p was completely identical among goat, mouse, rat, bovine, and even chicken, whereas differed in human (the 10^{th} A/ T) (Fig.1A). Although several studies unveil the adipogenesis-inducing function of miR-193b signaling [35, 36] and anti-tumor regulation of miR-193b in many cancers [17, 18, 37], intriguingly, expression levels of MIR193BHG in human skeletal muscle ranked second among 53 tissues (Fig.1B, upper panel; Supplementary Fig.S1). In particular, hsa-miR-193b-3p is highly dominant than that of hsa-miR-193b-5p (Fig.1B, lower panel). Using RNAs extracted from goat tissues and cultured MuSCs isolated from newborn goat longissimus dorsi (LD) muscle, we also found out that compared with other internal organs, extinguished miR-193b-3p levels were presented in goat muscles from embryos at 75 d of gestation (E75) and maintained the high levels at birth (Fig.1C). Besides, miR-193b-3p abundance continually increased in LD muscles from embryonic to newborn goats (Fig.1C). Moreover, miR-193b-3p levels were steady in MuSC culturing in GM but dramatically elevated when shifting to DM (Fig.1C). These suggest that miR-193b-3p most likely play critical roles in mammal skeletal muscle development.

To address the function of miR-193b-3p in muscle development, we first transfected miR-193b-3p mimic (mi-193b-3p, 5 μg/mL) into goat MuSC cultured *in vitro*. We found out that comparing with the control (mi-Ctrl), ectopic miR-193b-3p (almost 170 foldchange relatives to control, $p<0.001$) greatly upregulated mRNA levels of proliferation and differentiation myogenic genes, including PAX7 ($p<0.01$), PCNA ($p<0.01$), MyoG ($p<0.05$), MyHC ($p<0.10$) and myomaker ($p<0.05$, Fig.2A). Furthermore, protein levels of PAX7 and MyoG were quantified by using western blotting (WB), and the results confirmed that the abundance of myogenic proliferation and differentiation genes were significantly elevated in mi-193b-3p-treated cells (Fig.2B). Also, we employed CCK-8 and EdU assay to monitor the proliferation ability and found out that miR-193b-3p mimic greatly elevated OD value at 450 nm after transfected for 24 h to 72 h ($p<0.05$ or $p<0.10$, Fig.2C), and the EdU^+ cells also dramatically increased at 48 h ($p<0.01$, Fig.2D, left panel; Fig.2E). Moreover, the myotube formation was induced by miR-193b-3p mimic, as shown by increased the size/number of MyHC staining cells at d 7 of differentiation (Fig.2D, right panel). Contrarily, inhibiting miR-193b-3p (in-193b-3p, 100 nmol) downregulated myogenic genes expression by 30%~50% ($p>0.05$, Fig.3A, B), as comparing to the control (in-Ctrl). Consistently, gene abundance, myoblast proliferation, and myotube formation were also retarded by deficiency of miR-193b-3p, as shown by OD values (Fig.3C), the fold change of EdU^+ cells, and MyHC staining myotubes (Fig.3D, E). Because factors affecting cell viability, including autophagy and apoptosis, also play a critical role in cell proliferation and differentiation [38], we evaluated the mRNA level of the key autophagy-related gene LC3B (Microtubule Associated Protein 1 Light Chain 3 Beta) [39] and BECN1 (Beclin 1), as well as apoptosis-related Caspase1 [40]. We found out that only levels of LC3B and BECN1 transcripts were elevated by ~1.5 fold when overexpressing miR-193b-3p ($p<0.05$), while others were unaffected by perturbing miR-193b-3p (Supp Fig.2). These results confirmed that miR-193b-3p positively regulates myogenesis of MuSC, which may be mainly attributed to the activation of proliferation ability.

miR-193b-3p targets and induces IGF2BP1 expression

To systematically anchor the overall effect of miR-193b-3p on global gene expression in myoblast, we performed transcriptome profiling in MuSCs treated with miR-193b-3p mimic (mi-193b-3p, n=4) and blank control (mi-Ctrl, n=4). Total RNA was extracted, qualified (Supplementary Fig. S3A, B), and then sequenced to analyze protein-coding genes affected. Over 8.29 Gb clean bases were identified for each sample; the total_mapped reads and unique_mapped reads were as high as 97% and 94%, respectively (Supplementary Fig. S3C); PCA analysis suggests that these samples were expectedly distinguished into two groups (Supplementary Fig. S3D).

Among the detected 20,268 transcripts, 471 ones were differentially expressed (DE, padj<0.05, Fig 4A), and these DE genes were significantly enriched in molecular function GO terms, including several cell growth and cell cycle, as well as insulin-like growth factor binding (GO:0005520, Padj = 0.015, Fig 4B). Since insulin-like growth factors (IGFs) play critical roles in skeletal muscle hypertrophy and regeneration through interplaying with the myogenic regulator like MyoD and MyoG [41], we analyzed all 17 insulin family genes detected and found out that out of 14 miR-193b-3p-induced genes, IGF2BP1 was the most dramatically affected one (Fig 4C).

Moreover, we validated the transcripts levels using qPCR (Supplementary Fig.S 4 and Fig 5A), and confirmed that compared with IGF2 and IGF1R, IGF2BP1 transcripts were dramatically upregulated when overexpressing miR-193b-3p, while decreased when miR-193b-3p was inhibited (Fig 5A, left panel). Consistently, IGF2BP1 protein levels were greatly elevated by miR-193b-3p mimic (Fig 5A, right panel). Additionally, similar to the miR-193b-3p expression profile, IGF2BP1 was also highly accumulated in skeletal muscles from goat kids at E75 and newborn (Fig 5B), and increased when MuSC shifted differentiation (Fig. 5B). These suggest that miR-193b-3p is potentially activates IGF2BP1.

Generally, miRNAs regulate gene expression through miRNA-mRNA interaction through sequence complementarity [7]. To validate the association between miR-193b-3p and IGF2BP1, first of all, by using online software FINDTAR3 and BIBIServ2, we found out that IGF2BP1 was the most excellent gene targeted by miR-193b-3 with shallow free energy (Mfe= -32.50 kcal/mol) (Fig.5C). To confirm the importance of base pairing between miR-193b-3p and IGF2BP1, we inserted the wild and mismatch mutations downstream of Rinilla (R-Luc) to construct the wild type vectors (GGCCGG, R-Luc-IGF2BP1-wt) and the mutated ones (GTAAAG, R-Luc-IGF2BP1-mut) and transfected them into MuSC separately. As shown in Fig.5D, without miR-193b-3p, luciferase activity maintained similar among groups, including R-Luc-NC, R-Luc-IGF2BP1-wt, and R-Luc-IGF2BP1-mut; while the addition of miR-193b-3p mimic considerably activated R-Luc-IGF2BP1-wt luciferase activity ($p<0.001$), but caused no significant change in R-Luc-IGF2BP1-mut bearing seed-site mutations. Furthermore, in HeLa and C2C12 cells, we confirmed that 193b-3p substantially activated R-Luc-IGF2BP1-wt luciferase activity (Fig.5E). These results imply that IGF2BP1 is directly targeted and activated by miR-193b-3p.

Function of miR-193b-3p on myoblast proliferation is IGF2BP1-dependent

Previously reported that IGF2BPs，also named IMPs，participate development of many tissues through cell proliferation, especially HMGA2-IGF2BP2 axis is critical in regulating activation of satellite cells toward myogenesis [42]. To address the function of IGF2BP1 in myogenesis, we amplified the CDS of IGF2BP1 and constructed an overexpressing vector (pIGF2BP1, 3 μg/mL), as well as designed small interfering RNAs against IGF2BP1 (siIGF2BP1, 100 nM, Supplementary Fig. S5) and transfected them into MuSC separately. As shown in Fig.6A, ectopic IGF2BP1 (pIGF2BP1) dramatically promoted mRNA ($p<0.001$) and protein levels of IGF2BP1, while siIGF2BP1 resulted in ~20% downregulation of IGF2BP1 mRNA ($p<0.01$) but no dominant protein density altered, which mainly resulted from the deficiency of endogenous IGF2BP1 in cells. Moreover, pIGF2BP1-treated cells contained higher transcripts of Pax7 ($p<0.001$), MyoD ($p<0.01$), and MyoG ($p<0.001$), while deficiency of IGF2BP1 (siIGF2BP1) decreased all myogenic genes expression insignificantly ($p>0.10$) (Fig.6B). Additionally, the protein levels of PAX7 and MyoG elevated in pIGF2BP1-treated MuSCs confirmed the mRNA abundance altered (Fig. 6C). Correspondingly, EdU^+ cells were increased in pIGF2BP1 while decreased in siIGF2BP1 treated cells compared to the control group ($p<0.01$, Fig.6D). These results phenocopy overexpression or deficiency of miR-193b phenotype, respectively.

Furthermore, to validate whether function of miR-193b-3p is mediated by IGF2BP1, we transfected miR-193b-3p mimic (mi-193b-3p) and simultaneously interfering IGF2BP1 (siIGF2BP1) in MuSC. As shown in Fig. 6E, the abundance of PAX7 and PCNA were insignificantly altered ($p>0.05$) when IGF2BP1 deficiency, while transcripts of differentiation-related genes, including MyoD, MyoG, and Myomaker were still dramatically elevated ($p<0.05$). Furthermore, comparing with control, the fold change of EdU^+ cells at 24 h, 48 h, and 72 were insignificantly altered in cotransfected cells (Fig.6E, $p>0.10$), suggesting that instead of myogenic differentiation, the proliferation of myoblasts induced by ectopic miR-193b-3p cloud be efficiently reversed by IGF2BP1 deficiency.

Goat miR-193b-3p activates IGF2BP1 transcriptionally

To address the spatial localization of miR-193b-3p and IGF2BP1 mRNA in cells, we designed fluorescence-labeled oligonucleotide probes complementary to them and employed RNA-RNA dual-labeled fluorescence in situ hybridization (FISH). We found out that miR-193b-3p and IGF2BP1 mRNA were dominantly distributed and almost entirely colocalized in the cytoplasm of MuSC culturing in growth (GM 2d) and differentiation media (DM 7d, Fig.7A). Typically, over 84% of miRNAs bind complementary target RNAs and trigger their destruction [26]. To further monitor the effect of miR-193b-3p on turnover of endogenous IGF2BP1 mRNA, we treated culturing MuSCs with actinomycin D (ActD, 5 μg/mL) to compromise transcription effectively [43], and then quantified the remaining levels of IGF2BP1 transcripts at three sequential time points. Expectedly miR-

193b-3p mimic dramatically degraded IGF2BP1 mRNA in particular at 120 min ($p<0.01$), whereas interfering miR-193b-3p exhibited no effect on IGF2BP1 mRNAs stability (Fig.7B and Supplementary Fig. S6), just like the typical relationship between cytoplasmic miRNA and its targets [44]. These suggest that otherwise mechanism implicates in the activation of miR-193b-3p on goat IGF2BP1.

Currently, numerous mature miRNAs are identified in the nucleus [45], accompanied by several models unveiling transcriptional gene activation (TGA) closely related with the promoter and / or enhancer [31, 45, 46]. First of all, we quantified levels of mature miR-193b-3p in RNA samples separately extracted from the cytoplasm and nucleus of GM and DM myoblasts. Comparing with U6 snRNA (mainly nucleus-located) and 18s rRNA (dominant in the cytoplasm), a small part of miR-193b-3p was located in the nucleus, especially in GM myoblasts (GM 7.56 ±0.91 % vs. DM 2.73 ±0.54 %, $p<0.01$) (Fig.7C). Furthermore, using primers explicitly targeting IGF2BP1 heteronuclear RNA (hnRNA), we found out that ectopic miR-193b-3p (mi-193b-3p) efficiently unregulated IGF2BP1 hnRNA levels by ~4 fold as compared to its control (mi-Ctrl, $p<0.01$), while inhibiting miR-193b-3p did not alter IGF2BP1 hnRNA significantly (Fig.7D). These imply that the activation of miR-193b-3p on IGF2BP1 is possibly due to stimulating its transcription.

Furthermore, using data from UCSC, we found that compared with that in GM12878, H1-hESC, the hsa-miR-193b region in human skeletal muscle myoblasts (HSMM) is enriched with H3K4Me3 and H3K27Ac histone mark (Fig.7E upper panel, and Supplementary Fig. S7A), a signal used for a promoter and active enhancer discovery, respectively [47]. Moreover, TF factors such as YY1 (Yin and Yang 1) and CTCF (CCCTC-Binding Factor) that facilitates interactions including enhancer-promoter in a multi-gene cluster [48] are also enriched in hsa-miR-193b region (Data no shown). Whereas mouse miR-193b barely overlap with eRNA markers, including H3K4Me3 and H3K27Ac in limb from embryonic mouse aged 10 d (Supplementary Fig.S7B). On the other hand, both human and mouse IGF2BP1 3′ UTR region lack histone modification (Supplementary Fig. S8A, B), but the former enriches transcription factors including AGO2 (Argonaute RISC Catalytic Component 2), POLR2A (RNA Polymerase II Subunit A), CTCF (data not shown), suggesting that the activation of miR-193b-3p on IGF2BP1 is most likely attributed to the enhancer-related characteristics of goat miR-193b-3p.

To validate whether the goat miR-193b gene is enhancer-related, just like hsa-miR-193b-3p, we split it into two, amplified ~60 bp 5p and 3p region (Fig.7E lower panel), inserted them into a PGL3-Promoter vector separately (named pre-193b-5p and pre-193b-3p), and transfected these vectors into MuSC and HeLa. As shown in Fig.8F, comparing to the basic (pBasic) and control (pCtrl), pre-193b-3p efficiently promoted F-Luc/R-Luc levels in GM and DM myoblasts, as well as in HeLa cells ($p<0.01$ or 0.001), while miR-193b-5p enhanced F-Luc/R-Luc values greatly in DM cells ($p< 0.001$), implying that sequence of goat miR-193b could activate gene expression.

Another characteristic of activation-related miRNAs is its cis-activation on neighboring genes [31]. According to goat genome data, the adjacent genes for miR-193b include MKL2 (MKL/Myocardin Like 2), PARN (Poly(A)-Specific Ribonuclease), and BFAR (Bifunctional Apoptosis Regulator) (Fig.8A). So we quantified transcripts of these genes in goat MuSCs after perturbing miR-193b-3p, and found that in GM myoblasts, the expression of PARN and BFAR was induced by miR-193b-3p mimic, while deficiency of miR-193b-3p exhibited no significant effect on them; in differentiating cells, miR-193b-3p mimic elevated all these three genes mRNA levels, but miR-193b-3p inhibitor reversed these results ($p<0.1$, 0.05 or 0.01; Fig.8B). Furthermore, we amplified ~400 bp miR-193b region (pri-miR-193b) and overexpressed in MuSC, the levels of IGF2BP1 and PARN mRNA were significantly increased, compared with the control (pCtrl) ($p<0.01$, Fig.8 C).Also, disturbing miR-193b-3p failed to alter levels of miR-365-3p in goat MuSCs (Fig.8D, left panel), which is contradictory to the results in mouse C2C12 [24], because unlike some mammals including Homo sapiens, Mus musculus, and Bos taurus, miR-365 does not locate next to miR-193b in goat genome (Fig.8D, right panel, and Supplementary Fig. S9).

miR-193b-3p represses IGF2BP1 in mouse C2C12 myoblast

Although the mature sequence and the neighboring genes of miR-193b-3p are completely identical in goat and mouse (Fig.1A and Fig.8 A), previously reported that ectopic miR-193b blocks the shift of C2C12 myoblasts toward myogenesis [49]. To validate the function of miR-193b-3p in mouse myogenesis, we transfected the miR-193b-3p mimic (100 nmol) into mouse C2C12 myoblasts and found out that miR-193b-3p decreased IGF2BP1 mRNA levels ($p<0.05$); on the contrary, an inhibitor of miR-193b-

3p increased transcripts of IGF2BP1 ($p<0.10$; Fig. 9A), which is opposite to those in goat. Meanwhile, levels of cell number-related genes, including PCNA, cyclin D1, and caspase1 mRNA, did not change significantly (Fig. 9A). Furthermore, EdU^+ cells were also correspondingly downregulated in miR-193b-3p mimic treated cells or upregulated when deficiency of miR-193b-3p, as shown in Fig. 9B. Moreover, overexpression or deficiency of miR-193b generally failed to altered expression of its neighboring genes correspondingly, including MKL2, PARN, and BFAR, in GM and DM mouse C2C12 significantly (Fig. 9C). These results suggest that at least miR-193b-3p exhibited no activation on IGF2BP1 in mouse myogenesis.

Discussion

Muscle formation is precisely mastered by a handful of hierarchical gene cascades covering protein-coding genes such as MRFs as well as non-coding genes like miRNAs. It is well-accepted that miRNAs play critical roles in muscle development through inversely fine-tune gene enrichment canonically [8, 9]. Nevertheless, a few miRNAs have gained much attention for newly appreciated activation roles in directly targeted genes [50]. Here, we report that the anti-tumor gene miR-193b-3p induces proliferation and differentiation of goat MuSCs, phenocopying IGF2BP1 overexpression phenotype. Meanwhile, IGF2BP1 knockdown impairs myogenic proliferation but not differentiation of MuSCs induced by miR-193b-3p supplementation. Furthermore, miR-193b-3p in the nucleus directly targets 3′ UTR of IGF2BP1 gene and blooms IGF2BP1 abundance transcriptionally and overexpression of goat miR-193b-3p induces its neighboring genes. Besides, miR-193b-3p destructs IGF2BP1 mRNA in cytoplasm, which is in line with the inverse regulation of miR-193b-3p on IGF2BP1 transcripts in mics C2C12 myoblasts reported previously [24]. These results suggest that miR-193b-3p /IGF2BP1 axis exert activation in goat myogenesis which is mainly attributed to its nucleus function.

anti-proliferation vs. pro-proliferation function of miR-193b in muscle

In cancer tissues, miR-193b-3p functions oppositely as an anti-tumor [17, 51] or tumor-inducer [52] under differed disease conditions. As for the normal organ development, miR-193b–regulated signaling induces adipogenesis for adipose-derived stem cells (Mazzu, Hu et al. 2017, Mazzu, Hu et al. 2019) or even shifted from C2C12 cells [24]. On the contrary, deficiency of miR-193b induces cells from mouse BAT to the muscle lineage with upregulated levels of muscle-specific genes, including Cmk, Myf5, Myf6, MyoD, and MyoG [24]. Although muscle diseases like Duchenne muscular dystrophy 1 (DMD1) and DMD2 share similar symptoms, including gradually worsening muscle loss and weakness, miR-193b is accumulating in DMD1 patients [22] but downregulated in DMD2 [23], suggesting their miR-193b-related intrinsic mechanism differs. We found out that miR-193b-3p induces goat MuSCs proliferating and differentiating toward myotube, but using C2C12 myoblasts, we validate the suppressing effect of miR-193b-3p on myogenic proliferation reported previously [24]. Intriguingly, goat miR-193b-3p is predominantly located in the cytoplasm and triggers the destruction of IGF2BP1 mRNA, coinciding with the inverse regulation of mouse miR-193b-3p on IGF2BP abundance. Nevertheless, miR-193b-3p induces IGF2BP1 levels accumulating and goat MuSCs proliferating and differentiating toward myotube, which is differed from C2C12 myoblast. These suggest that cytoplasmic miR-193b-3p performs the canonical degradation of IGF2BP1 mRNA in myoblast but otherwise mechanism implicated in its activation on the goat IGF2BP1.

Activation of miR-193b on IGF2BP1 transcription

miRNAs are tacitly assumed as cytoplasm located and post-transcriptional negative regulators of its target gene expression[26, 27]. With the utilization of newly developed high-throughput assessment of miRNA, numerous mature miRNAs are currently identified in the nucleus [45]. Several models elaborating functions of nuclear miRNAs at both transcriptional (transcriptional gene silencing, TGS; transcriptional gene activation, TGA) have been constructed, in which miRNA targets and binds nascent RNA transcripts, gene promoter, or enhancer regions by a sequence complementary and exert further effects via recruiting additional epigenetic and(or) transcriptional factors or altering epigenetic modifications [45]. For example, miR-483-5p promotes the IGF2 transcription by targeting the P3 5′ UTR and promoter, accompanied by enrichment of activating-enhancer marks, including H3K4me3 and H3K27ac [32]. Similarly, the transcription activation of miR-373 on both E-cadherin [53], as well as miR-589 on *COX-2 (Cyclooxygenase 2)* [46], are via miRNA- promoter-related manner. Given the close relationship between gene enhancer and

promoter [54, 55], we speculate that most likely enhancer-related characteristics of miRNA-target pair, including enhancer-related miRNA or enhancer-related target, play a critical role in the activation of miRNAs on its target.

Currently, there are two distinct types of enhancer-related miRNAs: the super-enhancers (SEs)-miRNAs in which SEs neighbor cell-type-specific abundant miRNAs (like muscle-specific miR-1 and miR-133), boost pri-miRNA processing, and regulates mRNA stability [56]; the enhancer-overlapped-miRNAs including miR-26a-1, miR-339, miR-3179 and miR-24-1/2 that transcribed from enhancer region, exert enhancer activity including activating its neighboring gene expression in cis as well as global genes in trans via triggering its targeted enhancers [31]. Given that goat miR-193b-3p inducing IGF2BP1 through the complementary binding on its 3′ UTR that lack enhancer-related marks, we compared human and mouse data in the UCSC genome browser and found out that not the mouse but human miR-193b-3p gene locus is enhancer-overlapped (enriched with H3K27ac and H3K4Me3). Further, we found out that goat miR-193b-3p is partially nucleus-distributed and transcriptionally activates IGF2BP1 at both mRNA and protein levels, and this activation is completely abolished when mutated their base-pairing seed region. Besides, both pre-miR193b-5p and 3p could activate gene expression when inserted upstream of F-Luc, and both miR-193b-3p mimics and pri-miR-193b gene sequence promotes the expression of its neighboring genes, including MKL2, BFAR, and BFAR in GM and DM MuSCs, coinciding with the synergistic function and same phenotype between a mature miRNA and its passenger strand reported previously **[57]**. Nevertheless, in mouse C2C12 myoblast, miR-193b-3p negatively regulates IGF2BP1 abundance and barely affects its neighboring gene expression. These suggest that goat miR-193b-3p is most likely function as an enhancer-overlapped miRNA in myogenesis, and the difference of histone modification in the miR-193b gene region may be the main contribution for the species-related inconsistency of miR-193b-3p function.

Other factors possibly involved in miR-193b-3p/IGF2BP1 axis

IGFs play critical roles in myogenesis because they can uniquely promote muscle cell proliferation and differentiation, and induce MRFs mutually **[41].** In goat MuSCs treated with miR-193b-3p mimics, IGF2BP1 was the most dramatically affected IGFs gene. IGF2BP1 promotes proliferation in mouse embryonic fibroblasts [58], and IGF2BP2 mediates translation of myogenic proliferation genes [59]. Similarly, we found out that IGF2BP1 could induce myogenic proliferation and differentiation of goat MuSCs, while cotransfection results imply that miR-193b-3p/IGF2BP1 axis mainly affects proliferation. Given the many-to-many [60] and stage-specific [14] targeting manner between miRNAs and their targets**,** as well as other factors like the RNA A-to-I editing modification of miR-193b-3p [50] and m6A-dependent manner of IGF2BPs on the stability and storage of their target mRNAs [61], we speculate that part of these factors is likely involving in miR-193b-3p/IGF2BP1 pathway in promoting myoblast proliferation.

Conclusions

Taken together, here we proposed that similar to previously reported miR-24, the enhancer-overlapped miRNA-193b-3p carries a dual function ability: activating its target gene within the nucleus as well as repressing mRNA of the target gene in the cytoplasm. It is worth noting that miR-193b-3p in the nucleus exerts its function on promoting goat MuSCs' myogenesis by directly targeting 3′ UTR of the IGF2BP1 locus and inducing its expression, which is beyond previously reported models of nucleus-miRNA activation on targets [45]. Our research further extends the repertoire of miRNA functions.

Abbreviations

MuSCs: skeletal muscle satellite cells

CCK-8: cell-counting kit-8

EdU: 5-ethynyl-2'-deoxyuridine

FISH: fluorescence in situ hybridization

IGF2BP1: insulin-like growth factor-2 mRNA-binding protein 1

MRE: miRNA recognition element

UTR: untranslated region

hnRNA: heteronuclear RNA

Pax7: paired box 7

PCNA: proliferating cell nuclear antigen

MRFs: myogenic regulatory factors

MyoD: myogenic differentiation protein 1

MyoG: myogenin

myomiRs: muscle miRNAs

miRNAs: microRNAs

DMD: Duchenne muscular dystrophy

LD muscle: longissimus dorsi muscle

GM: growth medium

DM: differentiation medium

PCR: polymerase chain reaction

CDS: coding sequence

ACTB: Actin Beta

SDHA: Succinate Dehydrogenase Complex Flavoprotein Subunit A

PGK1: Phosphoglycerate Kinase 1

Hprt: Hypoxanthine Phosphoribosyltransferase 1

RIPA: radioimmunoprecipitation assay

MyHC: Myosin Heavy Chain

LC3B: Microtubule Associated Protein 1 Light Chain 3 Beta

BECN1: Beclin 1

IGFs: insulin-like growth factors

YY1: Yin and Yang 1

CTCF: CCCTC-Binding Factor

AGO2: Argonaute RISC Catalytic Component 2

POLR2A: RNA Polymerase II Subunit A

MKL2: MKL/Myocardin Like 2

PARN: Poly(A)-Specific Ribonuclease

BFAR: Bifunctional Apoptosis Regulator

DMD1: Duchenne muscular dystrophy 1

COX-2: Cyclooxygenase 2

Declarations

Author information

College of Animal Science and Technology, Sichuan Agricultural University, 211# Huimin Rd., Wenjiang District, Chengdu 611130, China

Li Li, Xiao Zhang, Hailong Yang, Xiaoli Xu, Yuan Chen, Dinghui Dai, Siyuan Zhan, Jiazhong Guo, Tao Zhong, Linjie Wang, Jiaxue Cao, Hongping Zhang

Correspondence to Li Li and Hongping Zhang

Ethics approval and consent to participate

All experimental protocols present here were strictly conducted following the Regulations for the Administration of Affairs Concerning Experimental Animals (Ministry of Science and Technology, China), and entirely approved by the Animal Care and Use Committee, Sichuan Agricultural University.

Consent for publication

Not applicable.

Competing interests

The authors declare that no any type of potential conflict of interest implicated.

Availability of data and materials

The accession number for the RNA sequencing data reported here is NCBI BioProject: PRJNA665306.

Funding

This research was financially supported by the National Natural Science Foundation of China (31802048 and 31672402).

Authors' Contributions

The study was mainly conceived by Li Li, Jiaxue Cao and Hongping Zhang. Xiao Zhang, Hailong Yang, Xiaoli Xu, Yuan Chen, and Dinghui Dai cultured cells and performed the experiments; Siyuan Zhan, Jiazhong Guo, Tao Zhong, and Linjie Wang participated in study design. Li Li drafted the manuscript, and all authors reviewed and contributed to the manuscript.

Acknowledgments

The authors thank Jianzhou Big-Eared goats farm (Sichuan province, China) for providing animals and helping sample collection; Novogene for performing the RNA sequencing.

References

1. Buckingham, M., *Myogenic progenitor cells and skeletal myogenesis in vertebrates*. Curr Opin Genet Dev, 2006. **16**(5): p. 525-32.

2. Kuang, S., M.A. Gillespie, and M.A. Rudnicki, *Niche regulation of muscle satellite cell self-renewal and differentiation.* Cell Stem Cell, 2008. **2**(1): p. 22-31.
3. Millay, D.P., et al., *Myomaker is a membrane activator of myoblast fusion and muscle formation.* Nature, 2013. **499**(7458): p. 301-5.
4. Tsai, W.C., et al., *Platelet rich plasma releasate promotes proliferation of skeletal muscle cells in association with upregulation of PCNA, cyclins and cyclin dependent kinases.* Platelets, 2017. **28**(5): p. 491-497.
5. Buckingham, M. and P.W. Rigby, *Gene regulatory networks and transcriptional mechanisms that control myogenesis.* Dev Cell, 2014. **28**(3): p. 225-38.
6. Paradis, F., et al., *Maternal nutrient restriction in mid-to-late gestation influences fetal mRNA expression in muscle tissues in beef cattle.* BMC Genomics, 2017. **18**(1): p. 632.
7. Pritchard, C.C., H.H. Cheng, and M. Tewari, *MicroRNA profiling: approaches and considerations.* Nat Rev Genet, 2012. **13**(5): p. 358-69.
8. Ge, Y. and J. Chen, *MicroRNAs in skeletal myogenesis.* Cell Cycle, 2011. **10**(3): p. 441-8.
9. Horak, M., J. Novak, and J. Bienertova-Vasku, *Muscle-specific microRNAs in skeletal muscle development.* Dev Biol, 2016. **410**(1): p. 1-13.
10. Batool, A., et al., *A miR-125b/CSF1-CX3CL1/tumor-associated macrophage recruitment axis controls testicular germ cell tumor growth.* Cell Death Dis, 2018. **9**(10): p. 962.
11. Haneklaus, M., et al., *miR-223: infection, inflammation and cancer.* J Intern Med, 2013. **274**(3): p. 215-26.
12. Mok, G.F., E. Lozano-Velasco, and A. Münsterberg, *microRNAs in skeletal muscle development.* Semin Cell Dev Biol, 2017. **72**: p. 67-76.
13. Zhan, S., et al., *A Novel Long Non-coding RNA, lncR-125b, Promotes the Differentiation of Goat Skeletal Muscle Satellite Cells by Sponging miR-125b.* Front Genet, 2019. **10**: p. 1171.
14. Li, G., et al., *miRNA-223 upregulated by MYOD inhibits myoblast proliferation by repressing IGF2 and facilitates myoblast differentiation by inhibiting ZEB1.* Cell Death Dis, 2017. **8**(10): p. e3094.
15. Lin, S.R., et al., *MiR-193b Mediates CEBPD-Induced Cisplatin Sensitization Through Targeting ETS1 and Cyclin D1 in Human Urothelial Carcinoma Cells.* J Cell Biochem, 2017. **118**(6): p. 1563-1573.
16. Wu, K., et al., *Deregulation of miR-193b affects the growth of colon cancer cells via transforming growth factor-beta and regulation of the SMAD3 pathway.* Oncol Lett, 2017. **13**(4): p. 2557-2562.
17. Hulin, J.A., et al., *MiR-193b regulates breast cancer cell migration and vasculogenic mimicry by targeting dimethylarginine dimethylaminohydrolase 1.* Sci Rep, 2017. **7**(1): p. 13996.
18. Streets, A.J., et al., *Parallel microarray profiling identifies ErbB4 as a determinant of cyst growth in ADPKD and a prognostic biomarker for disease progression.* Am J Physiol Renal Physiol, 2017. **312**(4): p. F577-f588.
19. Hummel, R., et al., *MicroRNA signatures in chemotherapy resistant esophageal cancer cell lines.* World J Gastroenterol, 2014. **20**(40): p. 14904-12.
20. Wang, F., et al., *Integrated analysis of microRNA regulatory network in nasopharyngeal carcinoma with deep sequencing.* J Exp Clin Cancer Res, 2016. **35**: p. 17.
21. van der Ree, M.H., et al., *Plasma MicroRNA Levels Are Associated With Hepatitis B e Antigen Status and Treatment Response in Chronic Hepatitis B Patients.* J Infect Dis, 2017. **215**(9): p. 1421-1429.
22. Perfetti, A., et al., *Plasma microRNAs as biomarkers for myotonic dystrophy type 1.* Neuromuscul Disord, 2014. **24**(6): p. 509-15.
23. Greco, S., et al., *Deregulated microRNAs in myotonic dystrophy type 2.* PLoS One, 2012. **7**(6): p. e39732.
24. Sun, L., et al., *Mir193b-365 is essential for brown fat differentiation.* Nat Cell Biol, 2011. **13**(8): p. 958-65.
25. Feuermann, Y., et al., *MiR-193b and miR-365-1 are not required for the development and function of brown fat in the mouse.* RNA Biol, 2013. **10**(12): p. 1807-14.
26. Baek, D., et al., *The impact of microRNAs on protein output.* Nature, 2008. **455**(7209): p. 64-71.

27. Guo, H., et al., *Mammalian microRNAs predominantly act to decrease target mRNA levels.* Nature, 2010. **466**(7308): p. 835-40.
28. Jangra, R.K., M. Yi, and S.M. Lemon, *DDX6 (Rck/p54) is required for efficient hepatitis C virus replication but not for internal ribosome entry site-directed translation.* J Virol, 2010. **84**(13): p. 6810-24.
29. Vasudevan, S., Y. Tong, and J.A. Steitz, *Switching from repression to activation: microRNAs can up-regulate translation.* Science, 2007. **318**(5858): p. 1931-4.
30. Orom, U.A., F.C. Nielsen, and A.H. Lund, *MicroRNA-10a binds the 5'UTR of ribosomal protein mRNAs and enhances their translation.* Mol Cell, 2008. **30**(4): p. 460-71.
31. Xiao, M., et al., *MicroRNAs activate gene transcription epigenetically as an enhancer trigger.* RNA Biol, 2017. **14**(10): p. 1326-1334.
32. Tang, S., et al., *MiR-483-5p promotes IGF-II transcription and is associated with poor prognosis of hepatocellular carcinoma.* Oncotarget, 2017. **8**(59): p. 99871-99888.
33. Noubissi, F.K., et al., *CRD-BP mediates stabilization of βTrCP1 and c-myc mRNA in response to β-catenin signalling.* Nature, 2006. **441**: p. 898.
34. Weber, G.F., *Molecular Analysis of a Recurrent Sarcoma Identifies a Mutation in FAF1.* Sarcoma, 2015. **2015**: p. 839182.
35. Mazzu, Y.Z., et al., *miR-193b–Regulated Signaling Networks Serve as Tumor Suppressors in Liposarcoma and Promote Adipogenesis in Adipose-Derived Stem Cells.* Cancer Research, 2017. **77**(21): p. 5728-5740.
36. Mazzu, Y.Z., et al., *miR-193b regulates tumorigenesis in liposarcoma cells via PDGFR, TGFbeta, and Wnt signaling.* Sci Rep, 2019. **9**(1): p. 3197.
37. Moore, C., J.K. Parrish, and P. Jedlicka, *MiR-193b, downregulated in Ewing Sarcoma, targets the ErbB4 oncogene to inhibit anchorage-independent growth.* PLoS One, 2017. **12**(5): p. e0178028.
38. Luo, Z., et al., *ROS-induced autophagy regulates porcine trophectoderm cell apoptosis, proliferation, and differentiation.* Am J Physiol Cell Physiol, 2019. **316**(2): p. C198-c209.
39. Lystad, A.H., et al., *Distinct functions of ATG16L1 isoforms in membrane binding and LC3B lipidation in autophagy-related processes.* Nat Cell Biol, 2019. **21**(3): p. 372-383.
40. Xi, H., et al., *Caspase-1 Inflammasome Activation Mediates Homocysteine-Induced Pyrop-Apoptosis in Endothelial Cells.* Circ Res, 2016. **118**(10): p. 1525-39.
41. Zanou, N. and P. Gailly, *Skeletal muscle hypertrophy and regeneration: interplay between the myogenic regulatory factors (MRFs) and insulin-like growth factors (IGFs) pathways.* Cell Mol Life Sci, 2013. **70**(21): p. 4117-30.
42. Li, Z., et al., *An HMGA2-IGF2BP2 axis regulates myoblast proliferation and myogenesis.* Dev Cell, 2012. **23**(6): p. 1176-88.
43. Lai, W.S., et al., *Inhibiting transcription in cultured metazoan cells with actinomycin D to monitor mRNA turnover.* Methods, 2019. **155**: p. 77-87.
44. Jonas, S. and E. Izaurralde, *Towards a molecular understanding of microRNA-mediated gene silencing.* Nat Rev Genet, 2015. **16**(7): p. 421-33.
45. Liu, H., et al., *Nuclear functions of mammalian MicroRNAs in gene regulation, immunity and cancer.* Mol Cancer, 2018. **17**(1): p. 64.
46. Matsui, M., et al., *Promoter RNA links transcriptional regulation of inflammatory pathway genes.* Nucleic Acids Res, 2013. **41**(22): p. 10086-109.
47. Sharifi-Zarchi, A., et al., *DNA methylation regulates discrimination of enhancers from promoters through a H3K4me1-H3K4me3 seesaw mechanism.* BMC Genomics, 2017. **18**(1): p. 964.
48. Ong, C.T. and V.G. Corces, *CTCF: an architectural protein bridging genome topology and function.* Nat Rev Genet, 2014. **15**(4): p. 234-46.
49. Washburn, M.C. and H.A. Hundley, *Controlling the Editor: The Many Roles of RNA-Binding Proteins in Regulating A-to-I RNA Editing.* Adv Exp Med Biol, 2016. **907**: p. 189-213.

50. Li, L., et al., *The landscape of miRNA editing in animals and its impact on miRNA biogenesis and targeting.* Genome Res, 2018. **28**(1): p. 132-143.
51. Zhang, J., J. Qin, and Y. Su, *miR-193b-3p possesses anti-tumor activity in ovarian carcinoma cells by targeting p21-activated kinase 3.* Biomed Pharmacother, 2017.
52. Zhong, Q., et al., *miR-193b promotes cell proliferation by targeting Smad3 in human glioma.* J Neurosci Res, 2014. **92**(5): p. 619-26.
53. Place, R.F., et al., *MicroRNA-373 induces expression of genes with complementary promoter sequences.* Proc Natl Acad Sci U S A, 2008. **105**(5): p. 1608-13.
54. Andersson, R. and A. Sandelin, *Determinants of enhancer and promoter activities of regulatory elements.* Nat Rev Genet, 2020. **21**(2): p. 71-87.
55. Weintraub, A.S., et al., *YY1 Is a Structural Regulator of Enhancer-Promoter Loops.* Cell, 2017. **171**(7): p. 1573-1588.e28.
56. Suzuki, H.I., R.A. Young, and P.A. Sharp, *Super-Enhancer-Mediated RNA Processing Revealed by Integrative MicroRNA Network Analysis.* Cell, 2017. **168**(6): p. 1000-1014.e15.
57. Shan, S.W., et al., *Mature miR-17-5p and passenger miR-17-3p induce hepatocellular carcinoma by targeting PTEN, GalNT7 and vimentin in different signal pathways.* J Cell Sci, 2013. **126**(Pt 6): p. 1517-30.
58. Dai, N., et al., *mTOR complex 2 phosphorylates IMP1 cotranslationally to promote IGF2 production and the proliferation of mouse embryonic fibroblasts.* Genes Dev, 2013. **27**(3): p. 301-12.
59. Gong, C., et al., *A long non-coding RNA, LncMyoD, regulates skeletal muscle differentiation by blocking IMP2-mediated mRNA translation.* Dev Cell, 2015. **34**(2): p. 181-91.
60. Sarver, A.L., L. Li, and S. Subramanian, *MicroRNA miR-183 functions as an oncogene by targeting the transcription factor EGR1 and promoting tumor cell migration.* Cancer Res, 2010. **70**(23): p. 9570-80.
61. Huang, H., et al., *Recognition of RNA N(6)-methyladenosine by IGF2BP proteins enhances mRNA stability and translation.* Nat Cell Biol, 2018. **20**(3): p. 285-295.
62. Zhao, W., et al., *The differential proliferation and differentiation ability of skeletal muscle satellite cell in Boer and Nanjiang brown goats.* Small Ruminant Research, 2018. **169**: p. 99-107.
63. Pisal, R.V., et al., *Detection of Mycoplasma Contamination Directly from Culture Supernatant Using Polymerase Chain Reaction.* Folia Biol (Praha), 2016. **62**(5): p. 203-206.
64. Li, L., et al., *MyoD-induced circular RNA CDR1as promotes myogenic differentiation of skeletal muscle satellite cells.* Biochim Biophys Acta Gene Regul Mech, 2019. **1862**(8): p. 807-821.
65. Qiu, L.Q., et al., *Measurement of mRNA Decay in Mouse Embryonic Fibroblasts.* Bio Protoc, 2016. **6**(13).
66. Love, M.I., W. Huber, and S. Anders, *Moderated estimation of fold change and dispersion for RNA-seq data with DESeq2.* Genome Biol, 2014. **15**(12): p. 550.

Figures

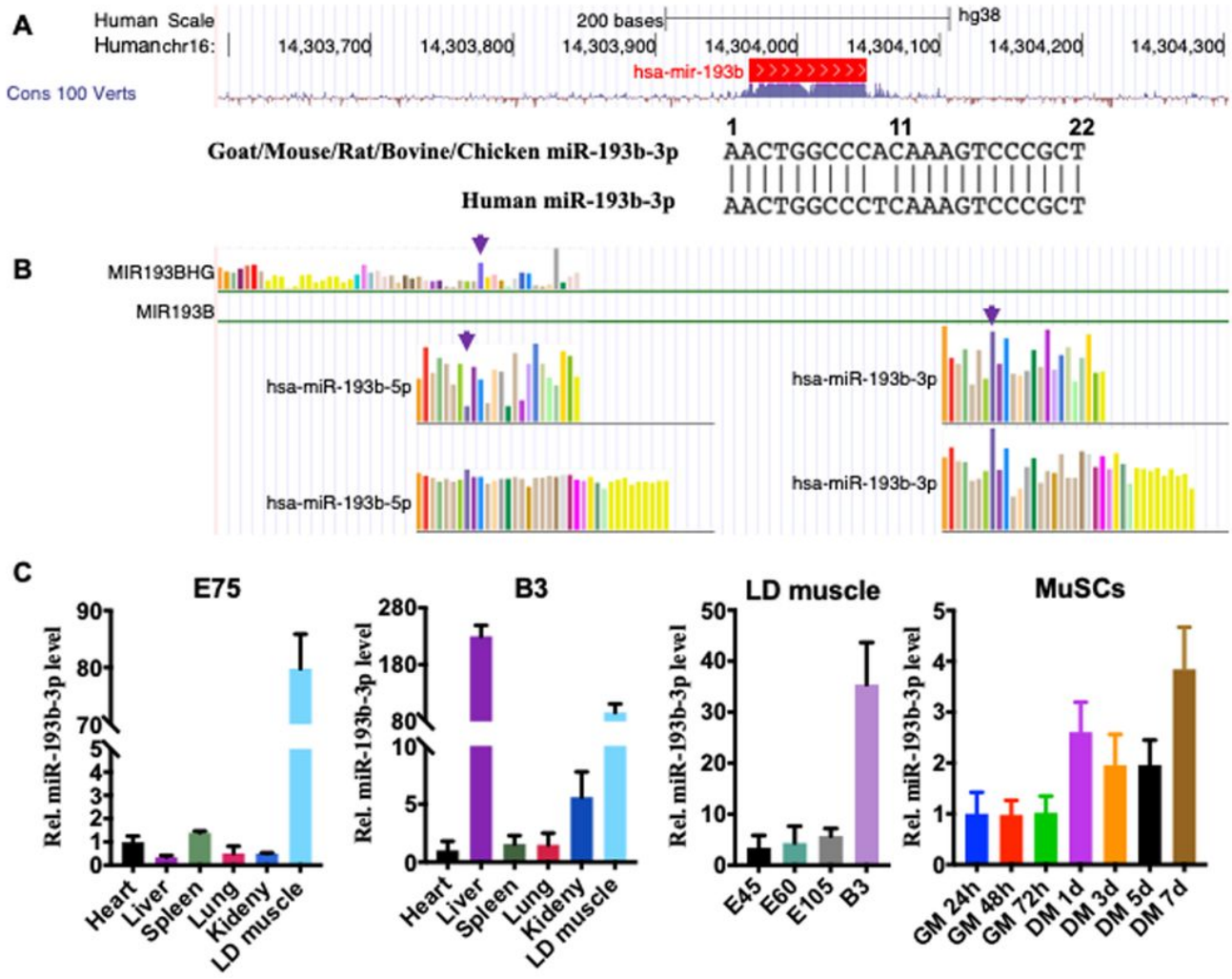

Figure 1

The sequence conservation and abundance of miR-193b-3p in human and goat tissues. A, miR-193b-3p is highly conserved among 100 verts in UCSC genome browser; the 10th nucleotide of human miR-193b-3p is different from that of other animals, including goat, mouse, rat, bovine, and chicken. B, expression of human MIR193BHG, miR-193b-5p, and miR-193b-3p in multiple tissues from GTEx. An arrow marks the skeletal muscle. C, levels of miR-193b-3p in tissues from embryonic 75 days (E75) and 3 d postnatal (B3) goat kids, or longissimus dorsi (LD) muscle from E45 to B3, as well as in cultured skeletal muscle satellite cells (MuSCs). RNA levels are quantified by employing RT-qPCR and calculated by the $2^{-\triangle\triangle Ct}$ methods, with normalization to β-actin (ACTB) and values of the first tissue or timepoint set to 1. Data are shown as mean ± SD (standard deviation).

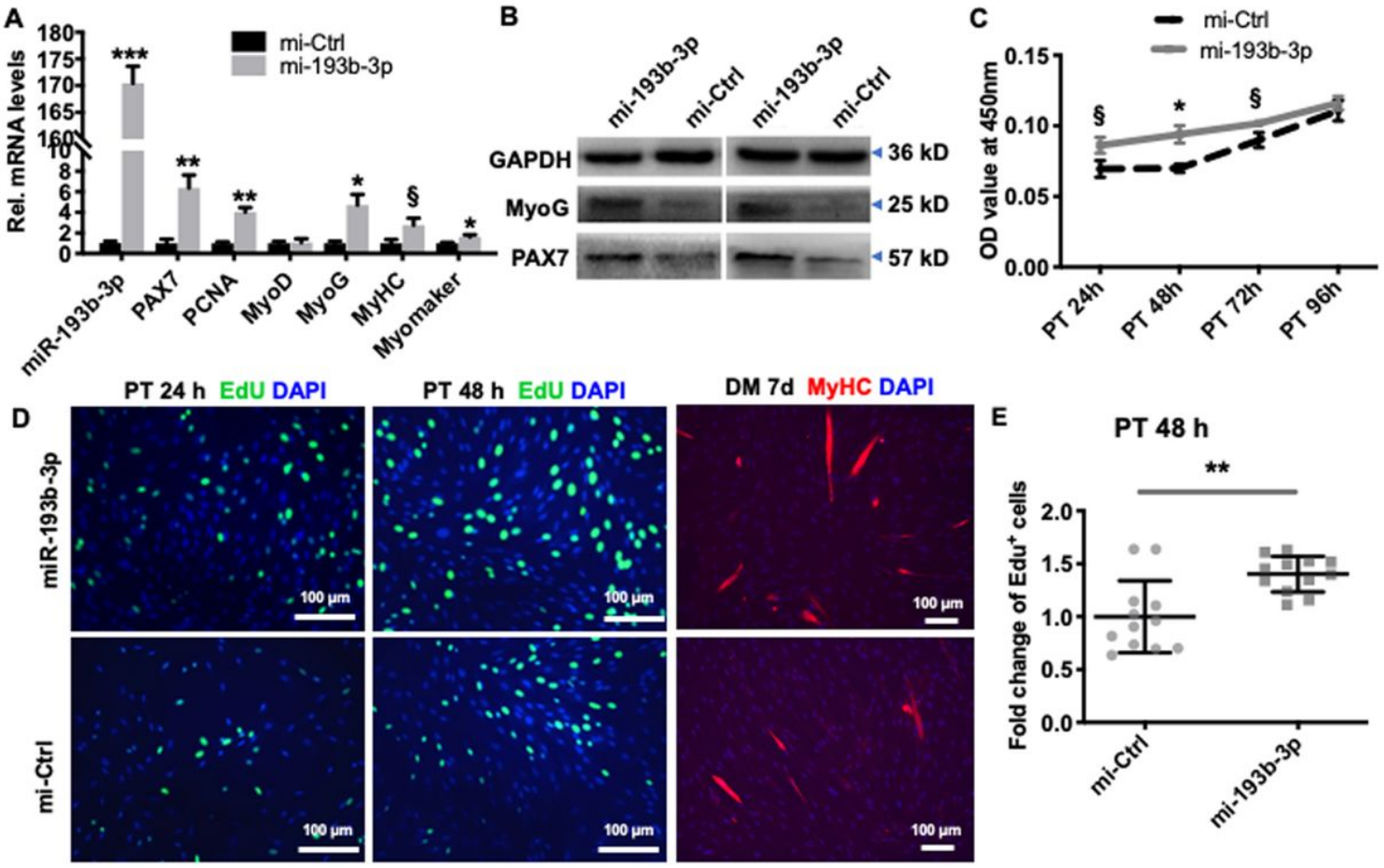

Figure 2

Overexpression of miR-193b-3p promotes the proliferation and differentiation of goat skeletal muscle satellite cells (MuSCs). A and B, miR-193b-3p elevates the abundance of myogenic genes. The cultured goat MuSCs were transfected with miR-193b-3p mimics or control (mi-193b-3p or mi-Ctrl, 50 nM), and cells were kept in growth media (GM) for 48 h or continually induced to differentiation for 48 h. The RNA levels of the target gene are quantified via RT-qPCR and calculated using the $2^{-\triangle\triangle Ct}$, with β-actin (ACTB) as an internal control and values of the mi-Ctrl set to 1. Using antibodies against PAX7, MyoG, and GAPDH (glyceraldehyde-3-phosphate dehydrogenase), western blotting (WB) assay was typically performed to detect protein levels of MyoD and MyHC in MuSCs treated with miR-193b-3p or mi-Ctrl. GAPDH works as a loading control. C, Cell proliferation is measured using Cell-Counting Kit-8 (CCK-8). Cells in 96-well plates (~2 × 103 cells per well) were transfected (mi-193b-3p or mi-Ctrl, 50 nM). And then every 24 h post-transfection (PT), the absorbance (OD) value at 450 nm is measured individually after adding 10 μL of CCK-8 reagents for 2 h. D, miR-193b-3p promotes EdU+ cells and myotube formation. Left panel, Representative immunofluorescence images of EdU and MyHC staining cells after transfected mi-193b-3p or mi-Ctrl (50 nM). Cells are cultured in GM consisting of 10 μM EdU, stained with anti-DAPI (blue) and anti- MyHC (red). Scale bar = 100 μm. Right panel, The EdU-stained cells (ratio of EdU+ myoblasts to all) are evaluated using randomly selected fields and normalized to control. Each treatment is at least tripled. Data are shown as mean ± SD. An unpaired two-tailed t-test is used to evaluate the means difference. Data are shown as mean ± SD. *** $P < 0.001$, ** $P < 0.01$, * $P < 0.05$, and § $P < 0.1$.

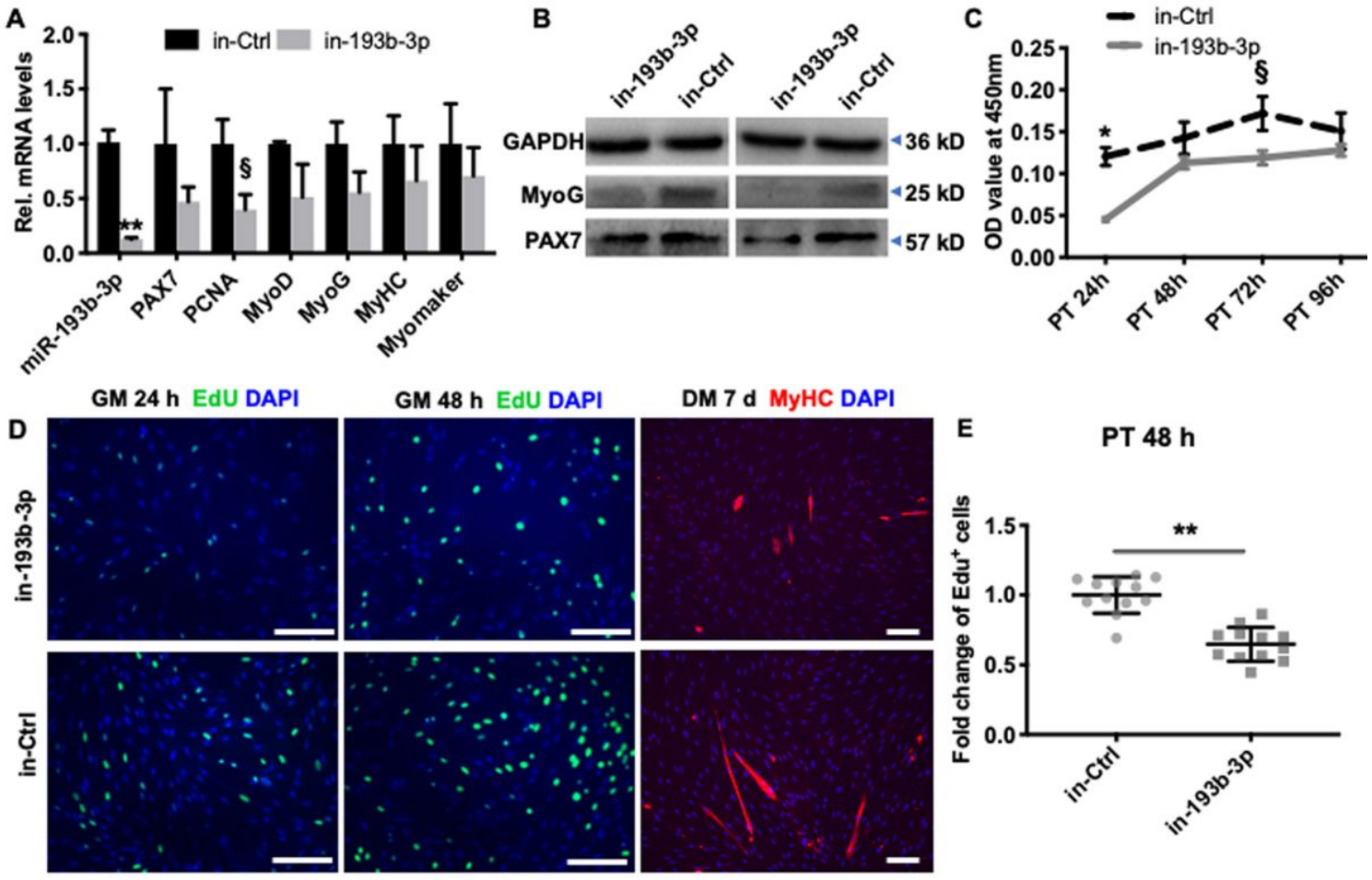

Figure 3

Deficiency of miR-193b-3p retards myogenesis of skeletal muscle satellite cells (MuSCs). A and B, deficiency of miR-193b-3p suppresses abundance of myogenic genes. The cultured goat skeletal muscle satellite cells (MuSCs) were transfected with interfering RNA against miR-193b-3p or control (in-193b-3p or in-Ctrl, 50 nM) when reached to ~50 % confluency. Then before be sampled to extract total RNA and protein, cells are kept in growth media (GM) for 48 h or induced to differentiation (DM) for 48 h. The RNA levels of the target gene are quantified via RT-qPCR and calculated using the $2^{-\triangle\triangle Ct}$, with β-actin as an internal control and values of the mi-Ctrl set to 1. Using antibodies against PAX7, MyoG, and GAPDH (glyceraldehyde-3-phosphate dehydrogenase), western blotting (WB) assay is typically performed to detect protein levels of MyoD and MyHC in MuSCs treated with in-193b-3p or in-Ctrl. GAPDH works as a loading control. C, deficiency of miR-193b-3p delays absorbance (OD) value of proliferation cells. Cells in 96-well plates (2 × 103 cells per well) are transfected (in-miR-193b-3p or in-Ctrl, 50 nM). Every 24 h post-transfection (PT), the absorbance (OD) value at 450 nm is measured individually after the addition of 10 μL of Cell-Counting Kit-8 (CCK-8) reagents for 2 h. D, deficiency of miR-193b-3p retards EdU+ cells and myotube formation. Representative images of EdU and MyHC staining cells transfected with in-193b-3p or in-Ctrl (50 nM). Cells are cultured in GM consisting of 10 μM EdU, stained with anti-DAPI (blue) and anti- MyHC (red). Scale bar = 100 μm. The EdU-stained cells are evaluated using randomly selected fields and normalized to control. Each treatment is at least tripled. Data are shown as mean ± SD. An unpaired two-tailed t-test is used to evaluate the means difference. Data are shown as mean ± SD. ** $P < 0.01$, * $P < 0.05$, and § $P < 0.1$.

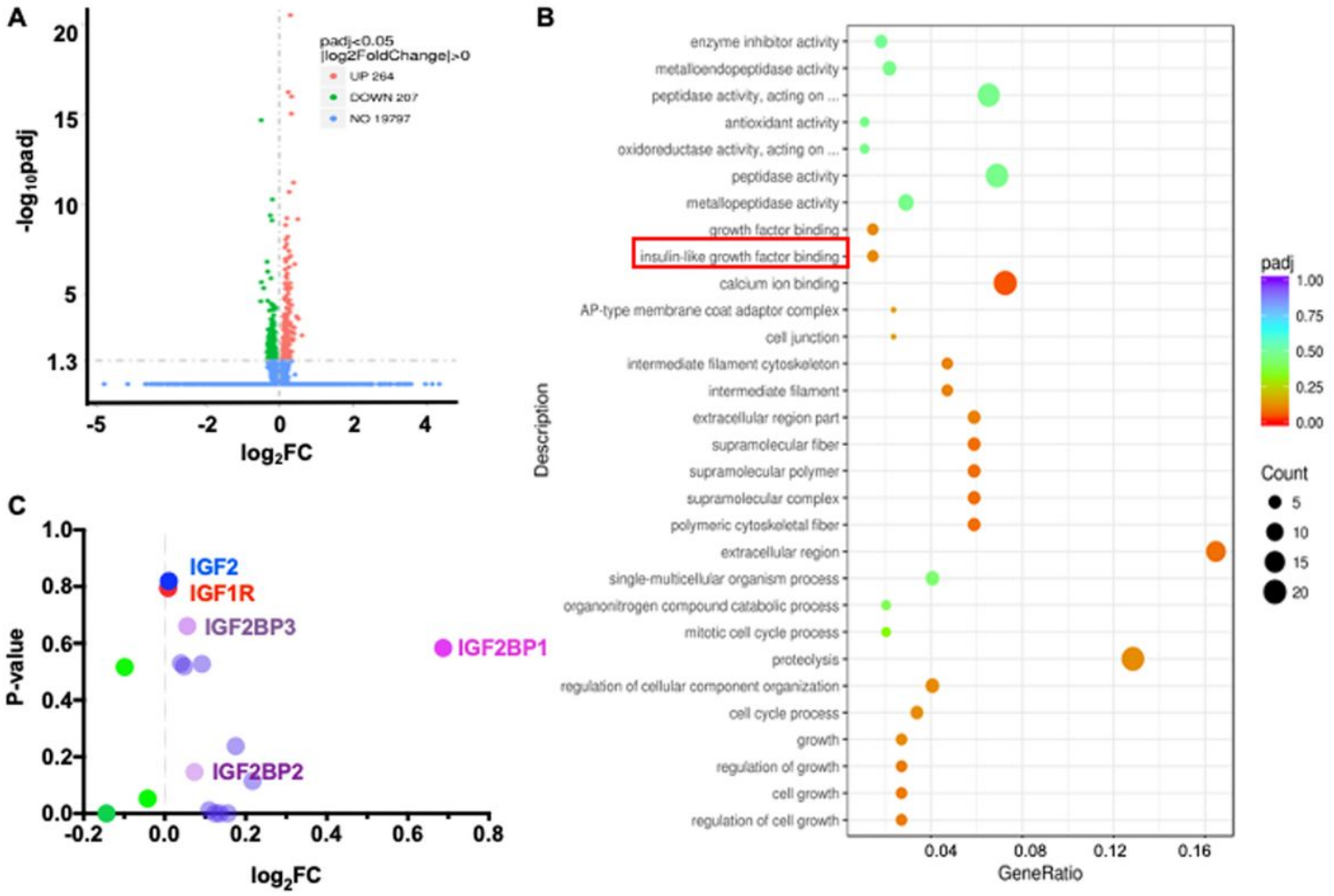

Figure 4

Insulin-like growth factor 2 binding protein 1 (IGF2BP1) is the most miR-193b-3p-affected insulin genes. A, a volcano plot displays log2foldchange (log2FC) against -log10padj from the t-test for all the transcript detected in mRNA-sequencing. B, Functional enrichment analyses of differential expression genes (DEGs) were implemented using the clusterProfiler R package (v. 3.4.4) with Padj < 0.05. A red box marks insulin-like growth factor binding (GO:0005520, Padj = 0.015). C, a volcano plot for the total 17 insulin family genes detected in RNA-seq. The green dot indicates that gene expression is decreased by miR-193b-3p mimics, while others are elevated compared to mimics control (mi-Ctrl).

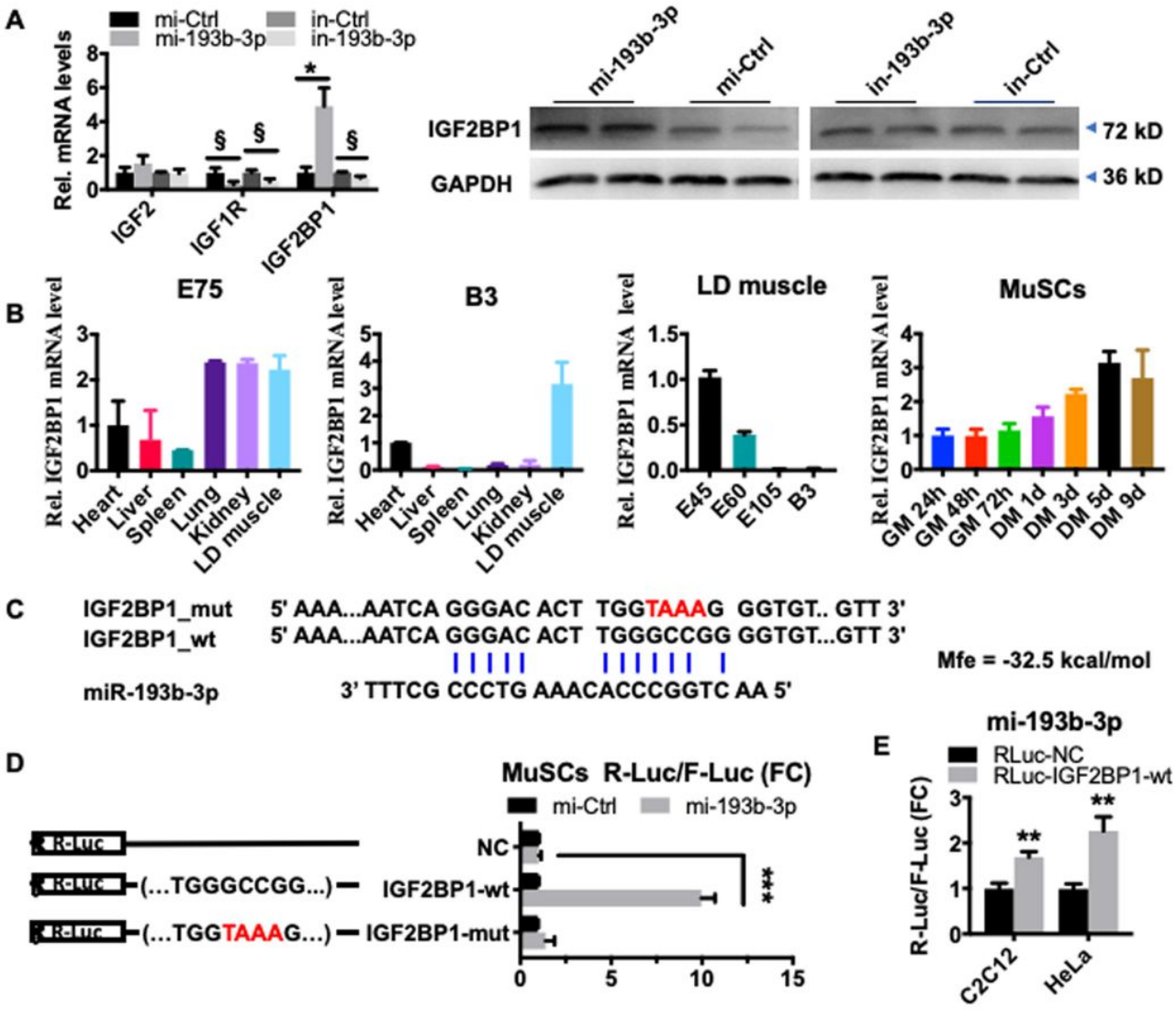

Figure 5

miR-193b-3p induces an abundance of insulin-like growth factor 2 binding protein 1 (IGF2BP1) through a seed-sites match. A, miR-193b-3p promotes IGF2BP1 abundance. The cultured MuSCs were transfected with 50 nM miR-193 mimics, mi-Ctrl, in-193b-3p, or in-Ctrl when reached to ~50 % confluency. Then cells were kept in GM for 48 h. The RNA Levels of IGF2, IGF1R, and IGF2BP1 were quantified via RT-qPCR and the 2−△△Ct, normalized to ACTB. Using antibodies against IGF2BP1and GAPDH, western blotting (WB) assay was performed to detect IGF2BP1 protein levels. GAPDH works as a loading control. B, the expression profile of IGF2BP1 in goat tissues is similar to that of miR-193b-3p. The mRNA levels IGF2BP1 are quantified by RT-qPCR and the 2−△△Ct methods, normalized to β-actin (ACTB), with values of the first tissue or timepoint set to 1. C, miR-193b-3p targets 3′ UTR of IGF2BP1. The potential seed match between miR-193b-3p within 3′ UTR regions of IGF2BP1 is predicted. The blue line indicates the complementary nucleotide. Mfe indicates free energy between IGF2BP1-wt and miR-193b-3p. D, the addition of miR-193b-3p activates luciferase activity of wild-type (R-Luc-IGF2BP1-wt) in MuSCs. The goat MuSCs (~1×104 cells per well) cultured in GM were cotransfected with blank control (NC), IGF2BP1-wt, or IGF2BP1-mut vectors, and miR-193b-3p mimics or control (mi-Ctrl) (640 ng/well for each vector). The activities of firefly and renilla luciferase were measured using a dual-luciferase reporter assay system. E, miR-193b-3p activates luciferase activity of R-Luc-IGF2BP1-wt in HeLa and mouse C2C12 myoblast. C2C12 myoblasts (~3× 104 cells per well) and HeLa cells (~2 × 105 cells per well) were cultured under similar conditions and transfection as goat MuSC. Data are shown as mean ± SD. An unpaired two-tailed t-test is used to evaluate the means difference. Data are shown as mean ± SD. *** P < 0.001, ** P < 0.01, and * P < 0.05.

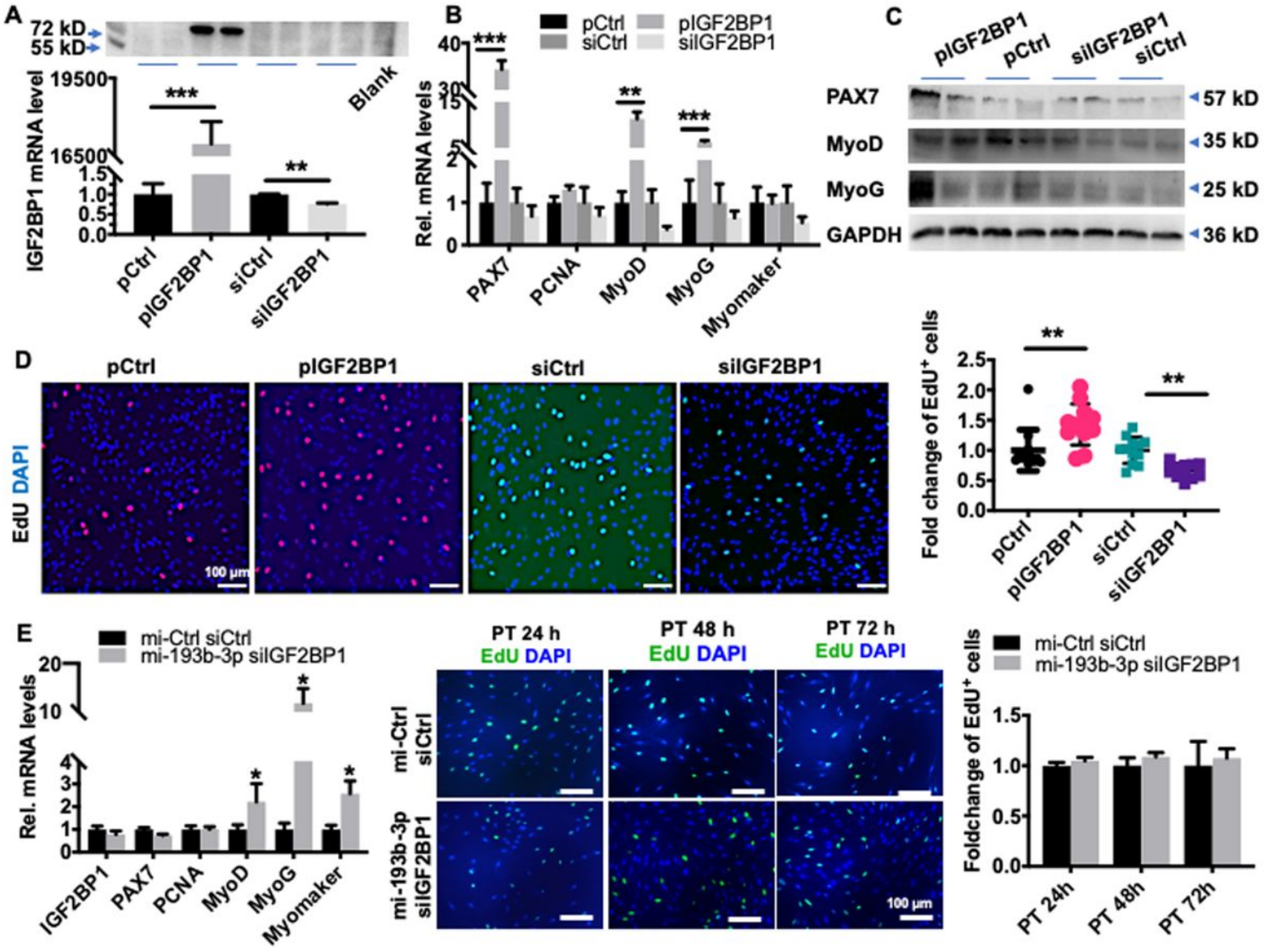

Figure 6

IGF2BP1 promotes myoblast proliferation. A, levels of IGF2BP1 are successfully disturbed. mRNA and protein levels of IGF2BP1 were measured in MuSCs 48 h post-transfection of pIGF2BP1(3 μg/mL) or siIGF2BP1(100 nM). The RNA Levels of IGF2BP1 were quantified via RT-qPCR and calculated using the 2−△△Ct. B and C, the effect of IGF2BP1 on myogenic genes. RNA levels were quantified via RT-qPCR and calculated using the 2−△△Ct, normalized to β-actin (ACTB), with values of control set to 1. Protein levels of PAX7, MyoD, and MyoG are quantified using typical western blotting (WB) assay, with GAPDH as a loading control. D, IGF2BP1 elevates EdU+ cells. Representative immunofluorescence images of EdU staining cells treated with pCtrl and pIGF2BP1(3 μg/mL, red) or siCtrl and siIGF2BP1(100 nM, green), cultured in GM consisting of 10 μM EdU (red or green) for 48 h, stained with anti-DAPI (blue). Scale bar = 100 μm. The fold change of EdU+ cells are evaluated using randomly selected fields and normalized to control. E, interfering IGF2BP1 retards miR-193b-3p-induced myogenic proliferation. Total RNA in cells cotransfected with miR-193b-3p mimics (mi-193b-3p, 50 nM) and interfering RNA against IGF2BP1 (siIGF2BP1,100 nM) or control were extracted 48 h post-transfection of in growth media (GM) or continually differentiated for 48 h (DM). RNA levels of target genes were quantified via RT-qPCR and calculated using the 2−△△Ct. Representative immunofluorescence images of EdU and DAPI (blue) staining cells post-transfection for 24, 48, and 72 h. Scale bar = 100 μm. The fold change of EdU+ cells are evaluated using randomly selected fields and normalized to control. Data are shown as mean ± SD. An unpaired two-tailed t-test is used to evaluate the means difference. Data are shown as mean ± SD. *** $P < 0.001$, ** $P < 0.01$, and * $P < 0.05$.

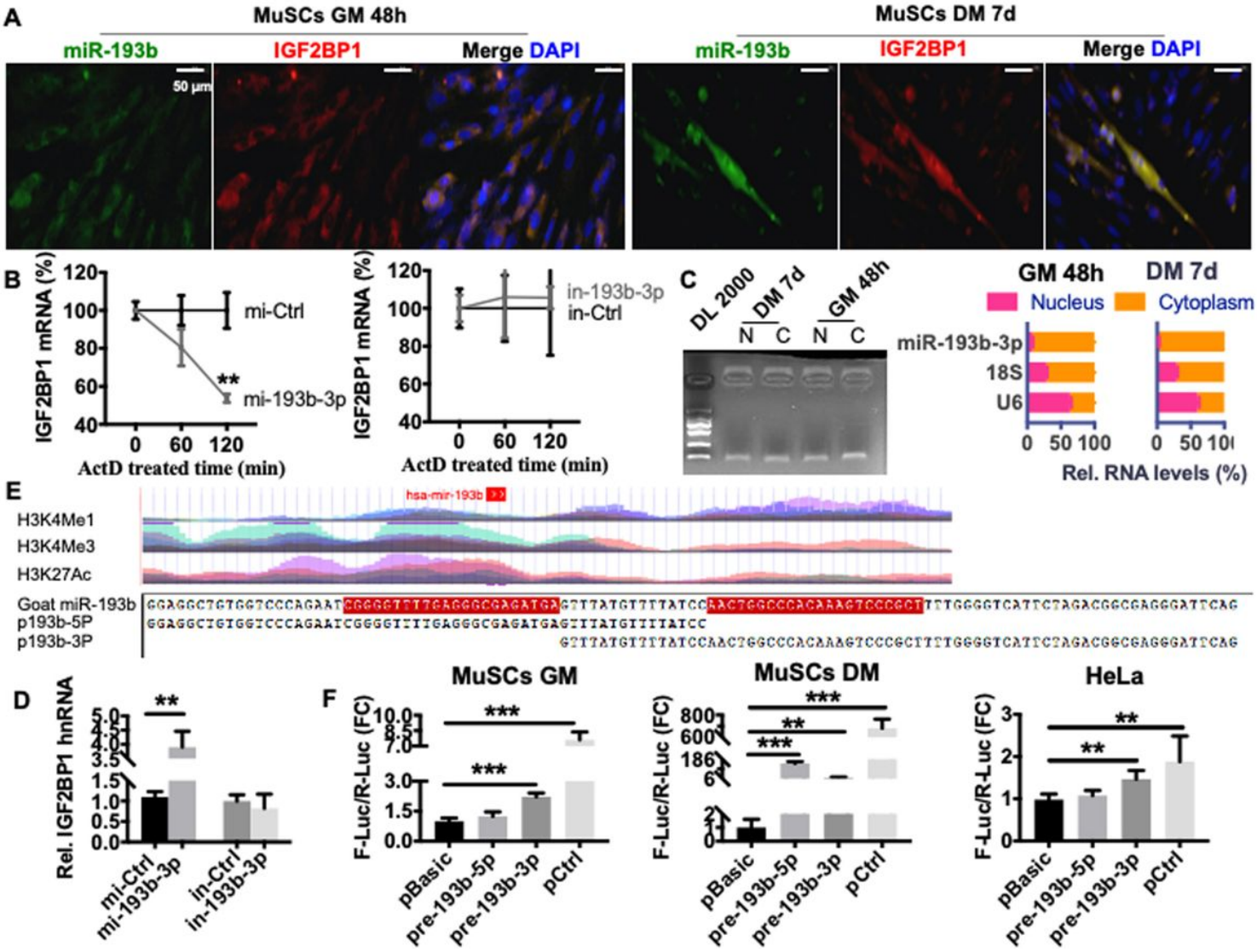

Figure 7

miR-193b-3p activates gene transcriptionally as an enhancer-related miRNA. A, colocalization of miR-193b-3p and IGF2BP1 mRNA. The Cy5-labeled probes target goat IGF2BP1 mRNA (red) and FAM-labeled chi-miR-193b-3p probes (green) are synthesized to localize them in MuSCs. The nucleus is stained with anti-DAPI (blue). Scale bar = 50 μm. B, miR-193b-3p degrades IGF2BP1 mRNA. MuSCs cultured in 12-well (~1 × 105 cells per well) plates are transfected with mi-193b-3p, mi-Ctrl, in-193b-3p, and in-Ctrl for 24 h. Cells were treated with ActD (5 μg/ml) and harvested at 0, 60, and 120 min. Finally, the remaining levels of IGF2BP1 mRNA were quantified using the canonical RT-qPCR method and calculated using the $2^{-\triangle\triangle Ct}$, with ACTB, SDHA, and PGK1 as an internal control. C, miR-193b-3p distributes in both cytoplasm and nucleolus. MuSCs proliferating for 2 d and differentiating for 7 d were fractionated into nuclear/cytoplasmic parts. The abundance of miR-193b-3p is quantified using RT-qPCR, presented in 1.5% agarose gels electrophoresis. N, Nucleus; C, Cytoplasm. D, miR-193b-3p promotes levels of IGF2BP1 hnRNA. MuSCs with disturbed miR-193b-3p abundance (miR-193b-3p, mi-Ctrl, in-Ctrl or in-193b-3p, 50 nM) for 48 h are harvested. Levels of IGF2BP1 hnRNA are quantified using RT-qPCR with specific primers located in intron and calculated using the $2^{-\triangle\triangle Ct}$. E, human miR-193b (hsa-mir-193b) locates in the enhancer region. Upper panel, hsa-mir-193b sits in the peak and valley of H3K4Me1/H3K4me3/ H3K27ac derived from 7 cell lines in ENCODE UCSC. Lower panel, the sequence of the goat miR-193b-3p gene. F, miR-193b sequence induces gene expression transcriptionally. Promoter vectors including pre-193b-3p, pre-193b-5p as well as the blank (pBasic) and control (pCtrl) (1.28 μg /mL) were transfected into MuSC and HeLa, F-Luc/R-Luc levels were measured 48 h post transection. Data are shown as mean ± SD. An unpaired two-tailed t-test is used to evaluate the means difference. Data are shown as mean ± SD. *** $P < 0.001$, ** $P < 0.01$, and * $P < 0.05$.

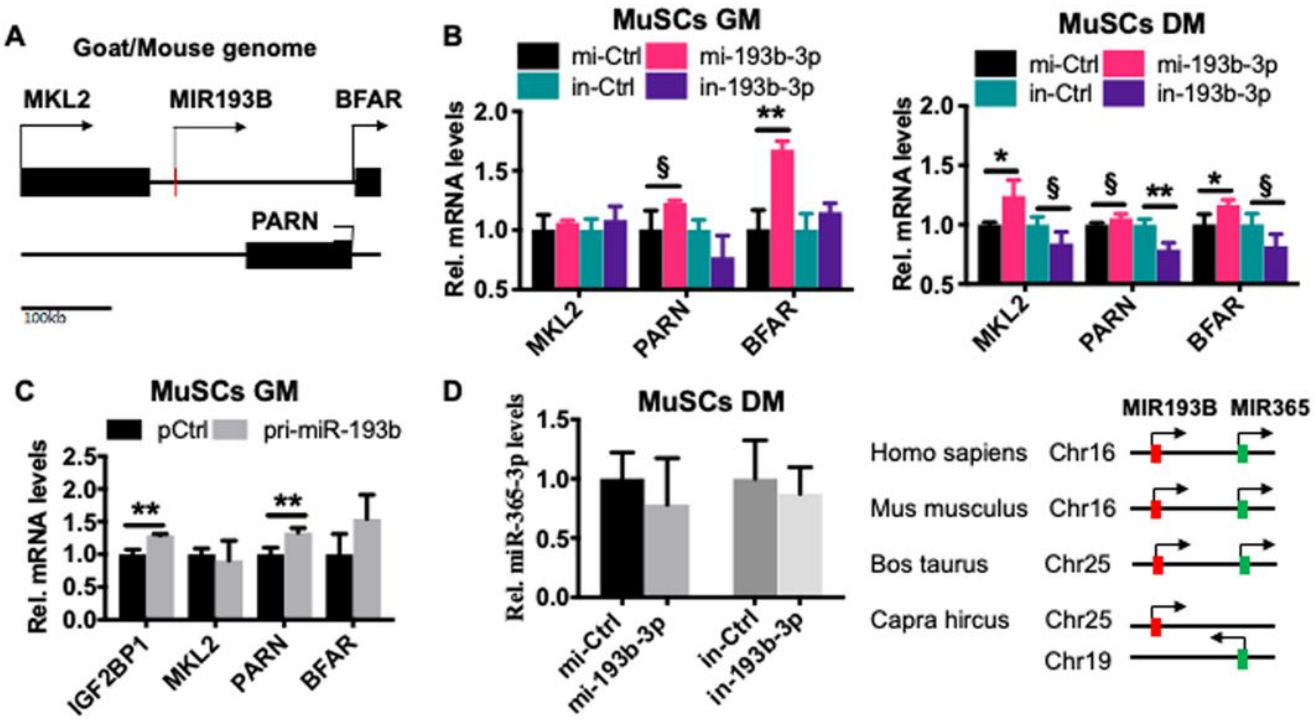

Figure 8

Goat miR-193b induces expression of its neighboring genes. A, neighboring genes of miR-193b-3p, including MKL2, BFAR, and PARN, are same in the goat and mouse genome. B, goat mir-193b induces expression of its neighboring genes. The transcripts of genes in miR-193b-3p-disturbed MuSCs cultured in GM and DM are quantified using qPCR. All values are normalized to geomean of ACTB, SDHA, and PGK1. The unpaired two-tailed t-test was used to evaluate the means difference. Data are shown as mean ± SD. ** $P < 0.01$, * $P < 0.05$, and § $P < 0.1$. C, Pri-miR-193b-3p activates the abundance of its neighboring genes and IGF2BP1. A fragment (~400 bp) containing miR-193b-3p is amplified and inserted into an overexpression vector, and then transfected into MuSCs cells. Cells are harvested 48 h later, and then the transcripts of target genes are quantified using qPCR. All values are normalized to geomean of ACTB, SDHA, and PGK1 value. The significance of means difference is evaluated using an unpaired two-tailed t-test. Data are shown as mean ± SD. ** $P < 0.01$. D, goat miR-193b-3p is unable to induce expression of miR-365-3p. Left panel, Disturbing miR-193b-3p in goat MuSCs fail to elevate transcripts of miR-365 (right panel). The unpaired two-tailed t-test was used to evaluate the means difference. Data are shown as mean ± SD. Right panel, miR193b (red box) and miR365a (green box) in human, mouse, and bovine are neighboring while in goat they are distributed on different chromosomes. An arrow marks the transcriptional direction of gene.

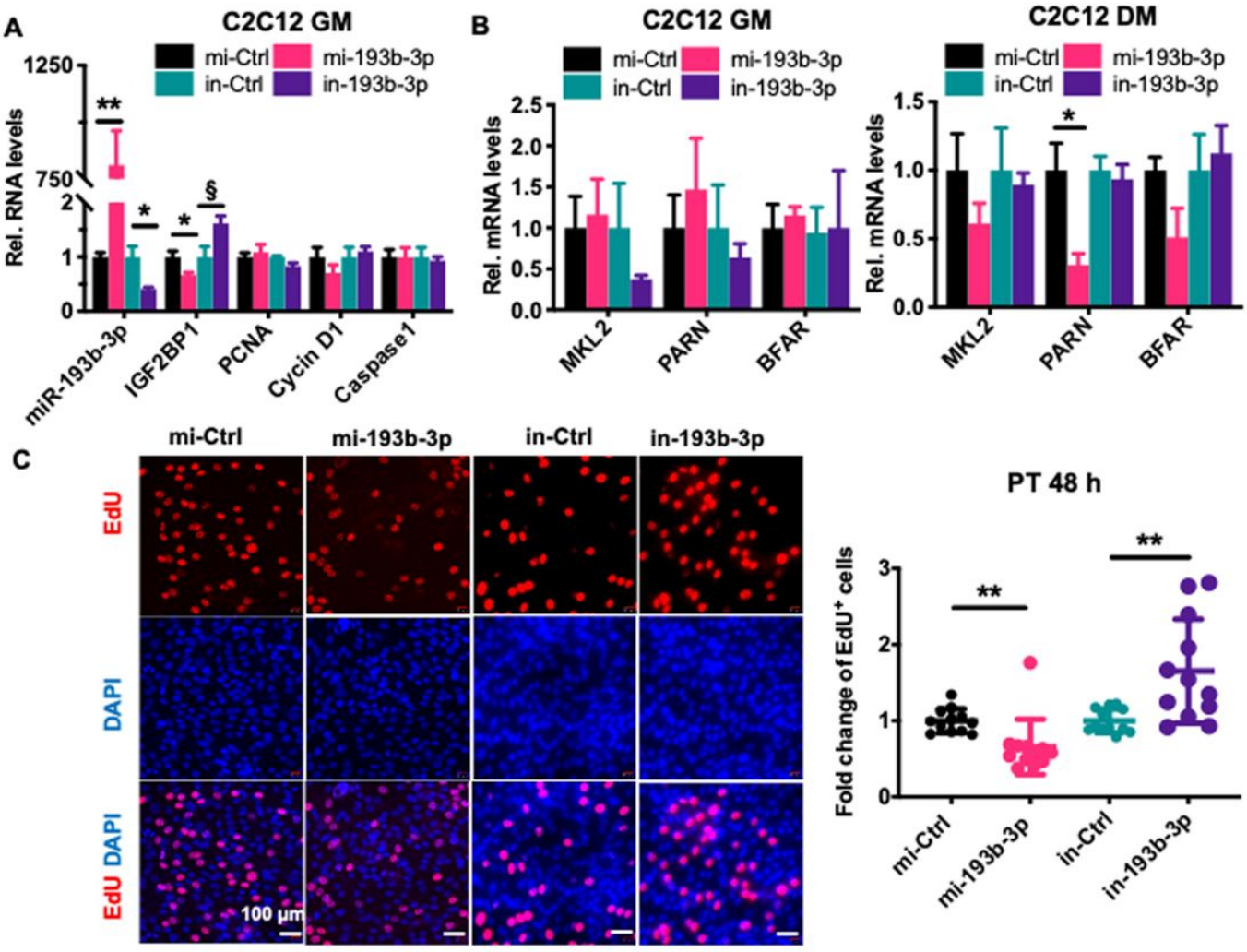

Figure 9

miR-193b-3p negatively regulates IGF2BP1 and suppresses the proliferation of mouse C2C12 myoblast. A and B, miR-193b-3p decreases transcripts of IGF2BP1 but barely affects the abundance of its neighboring genes in C2C12. RNA Levels of genes are measured in C2C12 transfected with miR-193b-3p mimic (mi-Ctrl and mi-193b-3p, 50 nM) or interfering RNA (in-Ctrl and in-193b-3p, 50 nM) for 48 h in GM or 48 h in DM with qPCR. All values are normalized to geomean of ACTB, GAPDH, and Hprt (Hypoxanthine Phosphoribosyltransferase 1). C, miR-193b-3p deduces EdU+ cells in C2C12. Representative immunofluorescence images of EdU staining cells in miR-193b-3p-disturbed C2C12 (mi-Ctrl and mi-193b-3p, in-Ctrl and in-193b-3p, 50 nM) (left panel). C2C12 are cultured in GM consisting of 10 μM EdU (red or green) for 48 h, then stained with anti-DAPI (blue). Scale bar = 100 μm. The fold change of EdU+ cells (ratio of EdU+ myoblasts to all) are evaluated using randomly selected fields and normalized to control. Each treatment is repeated ten times. Data are shown as mean ± SD. An unpaired two-tailed t-test is used to evaluate the means difference. Data are shown as mean ± SD. ** $P < 0.01$, * $P < 0.05$, and § $P < 0.1$.

Supplementary Files

This is a list of supplementary files associated with this preprint. Click to download.

- SupplementaryTable1.docx
- SuppFig.S9.tiff
- SuppFig.S8.tiff

- SuppFig.S7.tiff
- SuppFig.S6.tiff
- SuppFig.S5.tiff
- SuppFig.S4.tiff
- SuppFig.S3.tiff
- SuppFig.S2.tiff
- SuppFig.S1.tiff